3-2022

Analysis of Microscopic Carbon Fiber Fragments

Zachary R. Scott

Analysis of Microscopic Carbon Fiber Fragments

THESIS

Zachary R. Scott, Major, USA

AFIT-ENP-MS-22-M-109

DEPARTMENT OF THE AIR FORCE
AIR UNIVERSITY

AIR FORCE INSTITUTE OF TECHNOLOGY

Wright-Patterson Air Force Base, Ohio

AFIT-ENP-MS-22-M-109

ANALYSIS OF MICROSCOPIC CARBON FIBER FRAGMENTS

THESIS

Presented to the Faculty

Department of Engineering Physics

Graduate School of Engineering and Management

Air Force Institute of Technology

Air University

Air Education and Training Command

in Partial Fulfillment of the Requirements for the

Degree of Master of Science in Nuclear Engineering

Zachary R. Scott, B.S.

Major, USA

March 2022

AFIT-ENP-MS-22-M-109

ANALYSIS OF MICROSCOPIC CARBON FIBER FRAGMENTS

THESIS

Zachary R. Scott, B.S.
Major, USA

Committee Membership:

Abigail Bickley, Ph.D.
Chair

Darren Holland, Ph.D.
Member

Nina Sekerak, Ph.D.
Member

AFIT-ENP-MS-22-M-109

Abstract

Carbon Fiber (CF) has different tensile strengths and transverse moduli depending on how they are fabricated. Some CF is export controlled as it can be used for weapons, spacecraft, or gas centrifuges for enriching nuclear fuel. This research project focused on developing a reproducible method for preparing less than 300um length single CF threads in order to measure their transverse modulus. The end goal was to compare the transverse moduli of non-export controlled CF to that of an export controlled CF and annotate any characteristic similarities or differences. Five total polyacrylonitrile (PAN) fibers were used in this project, one of which was an export controlled fiber.

CF threads were separated from a 1 mm section of a CF tow with tweezers in a drop of water. These threads were then adhered to an Scanning Electron Microscope (SEM) disk with the use of a two-part epoxy. Once mounted, the threads were examined with a SEM to identify exposed threads, which can be tested using the Atomic Force Microscope (AFM). A Focus Ion Beam (FIB) was used to cut CF thread to less than 300 µm in length, if required, and also used to lightly ablate gross contamination, epoxy, or thread sizing that was present. This step was done to ensure it was the CF thread's modulus that was being measured and not residual adhesive or other contamination on the thread.

The prepared CF thread's transverse modulus was analyzed using a Bruker AFM in PeakForce Quantum NanoMechanics mode. Developing and applying selective criteria for all measurements to eliminate outliers for an individual CF thread's modulus produced the following key observations. First, the length of the fiber did not impact the measured modulus. Second, the export controlled CF thread had the least amount of measured variability in the transverse modulus by 0.74% to 3.34%

depending on which other thread was compared. Third, the export controlled CF thread had the least amount of skewness in its measured modulus distribution by a value of 0.2. (A normal distribution has a skew value of 0 and distributions in this project ranged from greater than 0 to less than 0.5). This observation suggests that a possible difference between export controlled and not controlled may not reside in the transverse modulus value of a CF thread, but rather, in the reduced amount of variation between measurements implying the overall uniformity of the export controlled thread is better than those produced for commercial purposes.

Acknowledgements

The author would like to acknowledge the assistance and advice of the members of his committee, this research would not have been completed with any degree of scientific standard without the support of Dr. Bickley, Dr. Holland, and Dr. Sekerak. MAJ Kemnitz must also be thanked as he proposed the idea and facilitated the inclusion of the Focus Ion Beam and Scanning Electron Microscope for this project. The author also appreciates the assistance of and support of the other AFIT nuclear engineering students, whose superior programming abilities and knowledge of software made much of this project's data presentation possible. Finally, the author must give a heartfelt thanks to his wife for understanding the long hours required and shouldering the majority of the household burdens in the final months of this research.

Zachary R. Scott

Table of Contents

Page

Page

List of Figures

List of Tables

ANALYSIS OF MICROSCOPIC CARBON FIBER FRAGMENTS

I. Introduction

1.1 Background and Motivation

Carbon fiber is one of the most diverse composite materials that has ever been developed. Its employment as a material ranges from road bicycle frames to space application purposes due to its strength, flexibility, weight, and high melting point [1]. As time has moved forward, carbon fiber has continued to be improved in all areas. What started out as an observation from experiments involving graphite deposits created by carbon arcs has grown into a full blown industry that continues to innovate and expand.

The first modern era carbon fiber was created in 1956 by Union Carbide, a company which was based outside of Cleveland Ohio. This material was discovered by Roger Bacon who was studying how carbon arcs behave when melting graphite at high temperature and pressure. The equipment was structured much like old carbon arc streetlamps were designed (Figure 1), but at much higher pressure and temperature. Bacon observed that the vaporized carbon would travel across the arc and then deposit on the opposite node as a liquid. After testing these small deposits he came to the realization that the carbon which had been vaporized and then reformed actually had amazing tensile and Young's modulus properties. The tensile strength is how much stress a material can absorb until it fails/breaks and Young's modulus is a material's resistance to elastic deformation or the stiffness of the material [2].

Figure 1 depicts how an arc lamp works, a current was run through two carbon

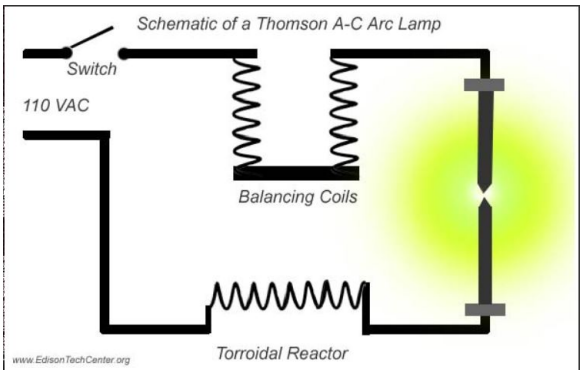

Figure 1. Schematic of an arc lamp. Reproduced by permission from Edison Tech Center [3].

tips that were then slowly drawn apart to maintain a low voltage arc between the two, illuminating the area around it. However, Bacon's carbon fiber was not a practical material as he was only able to make trace amounts of carbon fiber from this melted graphite. The jump in technology which truly revolutionized the industry came in 1959 when Curry Ford and Charles Mitchell created a method to produce sheets of fibers and cloth out of super heated rayon based carbon fiber. Not to be outdone, Bacon alongside Wesley Schalamon was then able to develop a revolutionary method of stretching carbon fiber 'yarn' under extreme temperatures to achieve an extremely high Young's modulus, something which had not been done before. This breakthrough demonstrated the correlation between the properties of carbon fiber and the way it was heat treated and stretched/prepared [2].

Though developments in carbon fiber strength and modulus continued to improve in small increments, Leonard Singer and Allen Cherry put themselves on the map in 1970 when they designed a 'taffy-pulling' machine for the stretching of carbon fiber. They waited until the CF was in a viscous mesophase, applied stress so that the individual molecules would align, and then applied heat to solidify the material, converting it to highly oriented carbon fiber. Not only was the carbon fiber extremely

strong, but it also now had thermal conductivity properties due to its molecular alignment [2]. This molecular alignment has been the key to developing stronger and more flexible carbon fiber. The more aligned the molecules become, the more the properties of the CF material can be tailored to specific requirements, the trick is to develop the techniques to achieve these results in a cost effective manner.

There are three basic forms of carbon fiber which have been mass produced, rayon, pitch, and polyacrylonitrile (PAN). Rayon-based carbon fiber, as mentioned above, was the first type of carbon fiber which was mass produced but currently represents less than 1% of carbon fiber currently in production. It is a cellulose based compound found in tree pulp that is then put through a series of basic and acidic baths before it is oxidized by heating to around 400 °C. After this procedure, the material is carbonized and graphitized and then stretched to improve the modulus. If the Rayon is not stretched there is a reduction on the order of one magnitude in the modulus. One of the reasons why this type of carbon fiber has gone out of style is because the production process is overall not as efficient or cost effective as the process for PAN or pitch-based carbon fibers [4]. Pitch-based carbon fiber is simply graphitized carbon that goes through the graphitization process between 1600-2800 °C. PAN-based carbon fiber is non-graphitizing carbon which never actually turns into graphite even after heating to 2000 °C. The graphite crystallization of the pitch based carbon fiber is what results in a high longitudinal modulus (or the ability to withstand stress without deforming), but generally a lower tensile strength when looking at high modulus fibers [5]. The ordered layers of carbon molecules in the PAN base fiber means the carbon atoms can align more tightly allowing for greater tensile strength (or the ability to withstand stress longitudinally without breaking), but generally lower longitudinal modulus (the ability resist elastic deformation longitudinally) [6].

Many industries today are interested in carbon fiber due to its low weight, high

strength, heat resistance, and ability to retain its original shape after experiencing a large amount of stress. Auto manufacturing, military, space, and recreational equipment industries all have enjoyed the benefits of using carbon fiber materials in their products due to its strength and weight. More specific to this current research project is the utilization of carbon fiber in nuclear weapons and uranium enrichment processes, more precisely its use within a gas centrifuge. A gas centrifuge has an internal rotor that is spinning at a very high rate of speed to leverage gravity and centripetal forces to separate isotopes. The heavier ^{238}U isotopes will move towards the outside of the cylinder (the gravitational bottom) while the lighter ^{235}U isotopes will move towards the axis of rotation (the gravitational top). In addition to moving in the x-plane, the isotopes will also travel in the y-plane with the heavier isotopes following gravity and moving lower while the lighter isotopes rise to the top. Because of this additional expected movement by the isotopes there are actually two scoops placed within the cylinder, one designed for the product, ^{235}U (located near the top and closer to the axis of rotation) and one for the tails, ^{238}U (located lower and closer to the outside wall). Figure 2 is a good representation of how a centrifuge works.

Although a gas centrifuge's rotor (the tube inside the casing that is the main component of the centrifuge and is responsible for spinning the materials inside) can be made out of a variety of materials such as maraging steel, or titanium, they only can achieve maximum rotational speeds of around 500 m/s or 440 m/s respectively. A carbon fiber rotor can achieve a rotational speed of about 720 m/s which means it is about 44% faster than maraging steel [8]. These numbers represent the peripheral speed of the rotor which is related to the maximum degree of isotope separation achievable by the centrifuge. Theoretically, this separation is thought to be the peripheral speed raised to the 4th power, but practically it is the peripheral speed squared. This means that even a slight improvement of the peripheral speed will

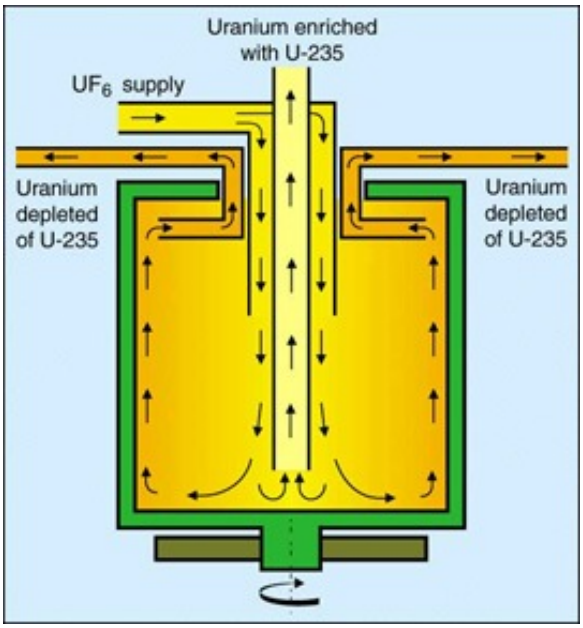

Figure 2. Representation of how a gas centrifuge works for the purposes of enriching uranium. Used with permission from the European Nuclear Society [7].

.

result in a larger increase in the maximum separation of isotopes [9]. (More time also will increase the quantity of material separated but for the purposes of this paper the best kind of centrifuge is defined as one that can separate material the most efficiently.) It is also important to note that carbon fiber development has improved since these numbers were recorded and some carbon fiber today can achieve higher rotational and subsequently peripheral speeds, but the exact numbers are not openly available [9][10][11].

Like most things physics related, gaseous centrifuge isotope enrichment is based on probabilities and statistics. Not all the ^{238}U isotopes will be uniformly spinning near the outside of the centrifuge, just waiting to be 'scooped.' Rather, there is a mathematical probability which statistically indicates the heavier isotopes will be near the outside and lower while the preference of the lighter ^{235}U isotopes will be closer to the axis of rotation and higher. The one variable which improves the chances of more

^{238}U isotopes drifting towards the outside is the speed at which the centrifuge spins. As discussed previously, there are several different materials which can be used in gas centrifuges, but since carbon fiber produces the fastest rotational speeds (highest centrifugal stresses) with the least amount of deformation, and risk of structural failure, it is now the preferred choice of material. In addition to being able to spin faster than either titanium or maraging steel, carbon fiber is also lighter which translates into less required energy input into the system to achieve the same amount of rotational speed. A carbon fiber centrifuge has the ability to spin at a rate of over 60,000 rpms, which correlates to the outside surface of that carbon fiber tube spinning many times over the speed of sound [8]. Both maraging steel and titanium rotors can not achieve this high of a speed and therefore will have a lower maximum separation ability for the uranium isotopes [9][11].

However, there are a plethora of different types of carbon fiber all with different qualities, meaning some carbon fibers can withstand more centrifugal force without deforming than others. This leads to the conclusion that within the realm of carbon fiber rotors some will be able to separate isotopes better than others. It also can be concluded that the higher the quality of the carbon fiber, the faster the rotor can spin, which means the faster uranium can be enriched.

1.1.1 Controlling the CF Supply

As more carbon fiber manufacturing techniques are developed and better carbon fiber is produced, there is the inherent responsibility attached to ensure the high quality carbon fiber is used appropriately by authorized countries. The use of carbon fiber for gas centrifuges is undeniable and the best quality material has become a controlled item worldwide. Nations, such as Iran, have attempted to acquire large amounts of carbon fiber, but without a clear explanation as to why they need it they

have been prohibited from buying it [12][13][14].

To this point the International Atomic Energy Agency has an agreement with all the member nations concerning equipment and supplies that are deemed to be export controlled. The Nuclear Suppliers Group (NSG) is a consortium that provides the supplies which are used in nuclear power and they work to ensure unauthorized countries do not acquire their products. Within the NSG there is a trigger list which essentially breaks down all aspects of the nuclear fuel cycle and outlines what equipment and materials are export controlled. Within that list is a section which outlines controlled items for centrifuges and specifically states that the controlled rotors spin at approximately 300 m/s or more and it further outlines export controlled rotors are maraging steel with a tensile strength of 1.95 GPa or greater and aluminium alloys having a tensile strength of 0.46 GPa. There is also a final note covering all other materials (such as carbon fiber) having a specific modulus of 3.18×10^6 m or a specific ultimate tensile strength of 7.62×10^4 m. The NSG defines the specific modulus as Young's modulus in N/m^2 divided by the specific weight in N/m^3 and the specific tensile strength as the ultimate tensile strength in N/m^2 divided by the specific weight in N/mm^3 [14]. Though it would be nice to have these limits in terms of in GPa, putting it in GPa would possibly make the list not inclusive enough. The best possible way to ensure all materials are controlled it associate the limits to each materials specific weight. With these specifications in place it enables the very tightly controlled nonproliferation environment which is in place today.

1.2 Research Objective

The objective of this work is to develop a method to reduce the size of a carbon fiber sample required to determine the relative transverse Young's modulus of a carbon fiber thread using an AFM. This objective will be achieved by completing three

subordinate objectives. Each supporting objective will impact the three stages of this research, sample preparation, data collection, and data processing.

1.2.1 Subordinate Objective One: Employing a Focus Ion Beam for Sample Preparation

A focused ion beam (FIB) will be employed for rastering a section of fiber to ablate off any type of gross contamination such as sizing or adhesive which may be found to cover it. The FIB will then be utilized to cut the length of the sample fiber to under 300 µm in length if the CF thread is not already short enough. This will enable the collection of data on a very small length of CF thread while minimizing any damage to the fiber that the use of bladed cutting instruments might have caused. At least one thread per CF type will be left longer than 300 µm to determine if length or cutting method has any impact on the measured modulus.

1.2.2 Subordinate Objective Two: Identifying Prepared Sections of CF Thread

Previous researchers have relied on using superglue to adhere the carbon fiber samples to an aluminum disk, but have had issues with being able to determine if the superglue had covered the sample or not [15][16]. To improve the chances of measuring a sample without adhesive covering it, a two part epoxy will be used and the sample will be observed with a SEM. Since the adhesive is an insulating material the bombarding electrons produce a charging effect, making the CF threads, which are covered by the adhesive, easy to identify. A 6000x microscope will also be utilized to ensure the proper location of the thread that has been exposed to the FIB is identified and marked in such a way it is easy to locate with the AFM's optics.

1.2.3 Subordinate Objective Three: Developing Selection Criteria for Data Processing

An important portion of this research project will be to distinguish data collected that is relevant and data which is theoretically erroneous or represents a non-real measurement. By ensuring measurements are near Gaussian, modulus measurements conform to theoretical expectations with respect to individual variables, and impossible outputs are summarily disregarded, it will be possible to ensure only data which is relevant will be used. To ensure measurements are near Gaussian a skewness test will be conducted on each modulus distribution collected and those distributions with a skew value less than -1.0 or greater than 1.0 will be discarded. Additionally, an ANOVA test will be conducted between the moduli values and the deformation height to ensure there is a correlation between the two. And finally, any negative height, indentation, or deformation values will be discarded since they would represent a non-real measurement. All of these tests and selection criteria will be crucial to the success of this research project.

II. Theory

2.1 Overview

In this chapter different methods past researchers used to characterize carbon fiber properties will be analyzed. Also, their findings will be linked to the current proposed method in an effort to pull out valuable data and insights. The primary focus of this research will be to reduce the sample size of a single carbon fiber strand to microns in length and investigate whether or not using a FIB to prepare a CF thread improves data collection through the use of an AFM.

2.2 Carbon Fiber (CF) Defined

It is important to define some terms associated with carbon fiber that are widely understood within the industry, explain how carbon fiber is fabricated, and give an overview of a CF thread's components from the inside out. The following sections will lay all of these objectives out and will give a good base of understanding for moving forward.

2.2.1 Carbon Nanotubes

The center, or core, of a the carbon fiber thread (one of the thousands which make up a tow) is made up of carbon fiber nanotubes which ideally run lengthwise in a very compact layered orientation. A nanotube is comprised of carbon atoms bonded together in a sheet (called graphene) and then wrapped to form a cylindrical shape. This creates a single-walled nanotube (SWNT). Concentrically aligning SWNT assemblies with a spacing about 0.34 nanometers creates multi-walled nanotubes (MWNTs) which have different corresponding properties than SWNTs [17]. As the name suggests, each nanotube is approximately a nanometer in diameter though

the true diameter of each nanotube varies and an entire carbon strand (also known as a thread in this paper) is approximately 2 µm in diameter so roughly 2000 nanotubes makeup a single carbon fiber thread. Not all production processes are perfect and sometimes the formation of the carbon nanotubes are not perfectly aligned in horizontal layers along the length of the CF thread. Carbon clusters (amorphous carbon) are one resulting defect. These carbon clusters are the carbon atoms bonded, not in a nice layered homogeneous manner, but rather bonded amorphously. [18]. This non-homogeneous shape can appear within the graphene or the nanotube formations themselves. In the next two sections a detailed explanation of the impact to the modulus and the tensile strength of the fiber when these clusters are present in large quantities is explored [17].

2.2.2 Nanostructure Impact on CF Strength and Modulus

Studies have been conducted using only PAN-based carbon fiber to investigate the correlation between the nanostructure of the PAN-based carbon fiber and the tensile strength of the fiber. It was determined that the CF could be broken up into different composites, carbon clusters, and carbon layers. Carbon clusters and carbon layering refers to the molecular structure of the fiber. Clusters, refer to the amorphous carbon-like component found in CFs (disordered carbon) whereas carbon layers refer to the graphitic component (ordered carbon) [19] [18]. The more uniform the carbon nanotubes are aligned, the stronger the material becomes in the aligned direction [20]. As with any material, the structure of the molecules is directly related to the density/strength of that molecule. Furthermore, it was observed that an increased carbon layer to carbon cluster ratio corresponded to a stronger fiber [19]. A research group was able to show that a distinct signature for carbon fiber, the ratio of predominately layered vs. predominantly clusters, exists. The more layered the carbon fiber

nanostructure the stronger the carbon fiber [19]. Another research group even went so far as to repair PAN CF with graphene and increased its tensile strength by reducing the overall amount of amorphous carbon in a sample [18]. If the nanostructure of the CF can be characterized by its carbon layer to carbon cluster ratio there is a hypothetical chance of differentiating between high modulus and low modulus carbon fiber. This follows from Chapter 1, where CF fabrication processes were developed to improve the alignment of the atoms/materials as they had a direct impact on the increase in material's modulus and strength [2]. Several research groups have used Raman spectroscopy for their study of CFs, and though this instrument will not be used in this research project, it is important to understand the relationship of the nanostructure of CF to its strength. The more graphene (ordered carbon) present the stronger it becomes [18].

2.3 Microstructure and Crystalline Size Impact on CF Strength and Modulus

Research has also been conducted which has looked at the microstructure and crystalline size of CF and tried to correlate those building blocks to the material's tensile strength and modulus. One particular research project looked specifically at how the transverse modulus of both PAN and pitch based carbon fiber compared to their tensile strength. It concluded that "the high ductility pitch-based, the high strength PAN-based, and the high modulus PAN-based single carbon fibers possess high compressive modulus and strength. In contrast, the high modulus pitch-based single carbon fiber possess low compressive strength and modulus" [21].

These researchers further explain that there is a correlation between the crystalline size and microstructure spacing to the actual strength of the carbon fiber. They used a Weibull distribution which is a statistical distribution usually used for predicting the

probability of material failure and applied it to CF. They discovered that when the interlayer spacing increased and the crystalline size decreased the transverse modulus decreased meaning that the sample was more resistant to elastic deformation with increased interlayer spacing and decreased crystalline size [21]. As in the previous section, this research project will not be pursuing the goal of linking the microstructure and crystalline size to the transverse modulus, but it is important to understand the variables which impact a CF thread's modulus.

2.3.1 Adhesive in CF

An important part of the CF fabrication process is the adhesive. An adhesive is used to bind the woven carbon fiber material together into a desired mold (see section 2.3.4. Choosing an adhesive is based on the type of sizing (discussed in section 2.3.3) used to coat the carbon fiber, the resin (discussed in 2.3.2) impregnated within the carbon fiber, and the intended use for the finished carbon fiber product. As with any material there are variances in quality and specifications for capability. Some carbon fiber composite products need to be more thermally resistant than strong and others need to be more flexible than strong. All of these variables factor into what type of carbon fiber tow is combined with what kind of adhesive, as well as the type of heat treatment used to bind the two together. The possibilities are nearly endless when looking at these variables, but choosing the correct adhesive is just as important as choosing the correct carbon fiber. Without the correctly paired adhesive, the carbon fiber composite fabrication process will ultimately fail to meet the desired specifications. The adhesive is noted here because it is imperative to understand that carbon fiber which has undergone the composite fabrication process will have additional variables impacting the modulus measurement. The finished carbon fiber thread will not be equivalent to a raw carbon fiber of the same type [22].

2.3.2 Resin in CF

Resin, like adhesive, is crucial to the structural integrity and strength the carbon fiber and its fabricated matrix. CF cannot be melted and molded by itself while retaining its strength/modulus identity, rather it has to be soaked in an adhesive that is tailored to bind with the resin and sizing with which that particular CF has been impregnated and coated with respectively [23]. Each carbon fiber is meant to be used with a certain type of adhesive based on its resin, and it is crucial that it is matched correctly. Though the resin is quite important for fabrication, it is also possible that it may impact the modulus measurements. However, it is hard to quantify how the resin would impact the modulus and how to account for the presence of the resin because of its uniform distribution throughout the CF thread. There is little that can be done to remove the resin for this project but it must be understood that the presence of the resin is an important feature in finished CF material, like a centrifuge rotor. In this case, the adhesive, resin, and fiber have been combined at extremely high temperatures to form the subsequent composite of interest. Once the resin, adhesive, and fiber bind together, the properties of the raw CF will have changed to that of the CF composite material. One research group looked at the implication of different adhesive/resin combinations and noted that although the tensile strength of the composite CF material is predominately based on the tensile strength of the CF itself; the matrix of the adhesive/resin which was formed sometimes added to the tensile strength, improving the overall performance of the material [23]. This theoretically could impact any modulus comparisons made between fabricated CF threads and raw CF threads of the same model/type. This note is important because the process, which is developed in this research project, may need to be applied to both fabricated and raw CF thread samples.

2.3.3 Sizing in Carbon Fiber

The term sizing for carbon fiber is a bit misleading as it immediately brings to mind a place in space, when it is actually about the coating on the fiber which protects the fiber from degradation during handling, transport, and storage. The sizing is also chosen based on its compatibility with the adhesive to be used to form the composite material. Some adhesive examples are epoxy, nylon, and urethane. These are used to bind the tows of CF together in the desired molded piece [24]. Sizing has many different chemical formulations based on the type of fiber it is being applied to as well as the company that is producing it. Generally though, sizing is comprised of "water, silane coupling agents, film formers, and a range of additives or modifiers such as surfacants, plasticizers, anti-static agents, antifoams, and rheology modifiers" [25]. Sizing may end up having an impact on the modulus measurements because the majority of the samples being tested in this project are cut from a tow of raw unprocessed carbon fiber. Thus, the presence of sizing on the majority of samples to be tested/measured in this project is certain. One method of removing sizing from fibers is acetone. However, one research group did find that treating CF with acetone lowered its flexural strength by 19%. Their method of treating was to soak the CF in acetone for 16 hours and then heat it to 100 degrees Celsius for 30 minutes to dry [26]. Flexural strength is related to modulus of the thread, the amount of resistance the thread has to elastic deformation. The only other way that the sizing can be removed is through heat treating at very high temperatures, which is impractical for this research project and also reduces the flexural strength by roughly 29% [27]. Removing the sizing is impractical with these two methods but there have been no studies conducted on whether or not a FIB could be used to remove sizing from CF. This research project will attempt to ablate any sizing that may be visually present on the CF thread. However, as the sizing is intended to adhere to the thread, some

of the chemical makeup of the sizing may have impregnated the thread to such an extent it has become part of the actual thread. Fabricated CF material will have had this sizing burned off or otherwise indistinguishably combined with the adhesive during the fabrication process which means real world samples would not have a detectable presence of a separate sizing layer. Consequently, the raw CF thread moduli values measured may not be comparable to finished CF thread moduli values as there will be the difference in the pre-fabrication composition of CF and post-fabrication composition of CF as it pertains to the presence of sizing. Thus, this research may be able to prove a working method for removing sizing from raw CF threads using a FIB.

2.3.4 Carbon Fiber Tow Fabrication Process

Now that the components of raw CF have been discussed, it is easier to give an overview of the overall fabrication process of CF material. Thousands of carbon fiber threads are wound and stretched together to create a tow of carbon fiber which is the form in which carbon fiber is distributed. The processes of winding and stretching is not unlike the processes used for spinning yarn. Tows are wound on a spool and distributed to manufacturing plants where they are then woven together much like a blanket or a sheet in a textile mill. The goal is to create a material that can easily be placed into a mold. For the purposes of this research project, it is important to make a distinction between carbon fiber that has undergone a fabrication process to become a composite material and raw carbon fiber. The fabrication of the carbon fiber composite material refers to when the weaved raw carbon fiber sheet is placed into a mold, soaked in an adhesive (to bind all the individual tows in the sheet together), and then baked at extremely high temperatures to create the desired strong, lightweight, and thermally resistant product. A finished CF sample refers to a sample obtained

from an object which has undergone the composite fabrication process. A raw sample refers to a single carbon fiber thread, pulled from a tow, that has not yet been used to fabricate any kind of product. The following sections will now go into detail regarding the composition of an individual CF thread [24][22].

2.3.5 Summary of CF Components and Fabrication Process

In the previous subsections it was outlined how CF was fabricated and how integral each component of a CF thread is to the final CF product. For the purposes of this research, substances such as sizing and resin could potentially impact the relative measurements of the actual CF thread. The impact of sizing on the measurement of the relative transverse modulus will be assessed by measuring fiber threads that have been exposed to a FIB and those of the same formulation that have not been exposed to a FIB. Though the presence of sizing is still likely regardless if it is visually observed the FIB should theoretically remove the majority of it.

2.4 Moisture Contents Influence on CF Strength

It has been shown that a common cause for weakening in carbon fiber is the amount of moisture the carbon fiber absorbs [28]. This degradation is combated by the sizing and the resin with which the carbon fiber is coated and impregnated. However, even with the reduction in water absorption, the CF water content will never be zero because of atmospheric influences. One research group used Raman spectroscopy to investigate the impact submerging carbon fiber tows in water had on its tensile strength and found a 7.5% to 10% decrease in the Young's modulus after being submerged for 300 days in demineralized or seawater respectively [29]. This conclusion gives a good basis to assume that the water absorption in carbon fibers in this project is probably not enough to appreciably perturb the modulus

measurements. The moisture to which the carbon fibers have been exposed is within the realm of moisture found in climate controlled office building in Ohio, not a tropical climate or an open air climate. Additionally, all AFM measurements will be conducted in a sealed box where the moisture and oxygen levels are controlled to less than 0.1 ppm and all samples will be allowed to dry in this box for 24 hours prior to testing to further eliminate any variation associated with moisture.

2.5 Focused Ion Beam (FIB)

This research project will use a FIB to raster and cut CF thread samples. Rastering is simply the passive ablation of material that occurs when the FIB is just viewing an object/sample. Much like a Scanning Electron Microscope (SEM) shoots electrons that interact with the object/sample and produce secondary electrons, backscattered electrons, and characteristic X-rays to produce an image, the FIB does the same thing, but with positively charged gallium ions. In viewing mode, the FIB bombards an object/sample with positively charged ions which also produces secondary and backscattered electrons, which are converted into images. However, due to the ions not being focused in a small area, the ablation is minimal. When the FIB is used to cut, these Ga^+ ions are focused on a small area to ablate the object/sample's material quickly and effectively. This cutting or ablation of the surface is due to 'sputtering' which is the phenomenon in which particles are ejected from a solid after it has been hit with energetic particles [30]. Unlike an SEM which bombards an object/sample with nondestructive electrons to create an image, a FIB imparts Ga^+ ions which interact with the surface and, because of conservation of momentum, can eject secondary ions, neutral atoms, as well as secondary electrons. The secondary electrons allow one to see an image as the sample is being rastered while the secondary ions and neutral atoms leaving the material are the actual ablation taking place [31]. Many research

groups have used FIB milling methods to expose the center of a carbon fiber thread without compromising the integrity of the thread structure with a mechanical sharp instrument such as a knife or scissors [32, 33, 21, 34, 35]. The FIB is very accurate and can mill objects with nm precision. Originally designed for preparing samples for a SEM, the FIB has become the preferred instrument when looking for a way to finely shape or cut a material. However, potential issues with the FIB include altering the atomic structure and heating the substrate through the intense bombardment of gallium ions, which can induce a cascade effect of destruction on the sample. The risks are theoretically minimal and the electron emissions from the sample as it is being ablated gives the ability to view the sample to ensure even ablation of the surface. The FIB offers this research project a reliable way to be able to prepare a single CF thread with an evenly ablated section due to its precise nature. Having a homogeneous section to measure will reduce the amount of error associated with any contamination, debris, sizing, or resin that may be inadvertently measured on the outside of the CF thread. It also should be noted that this technique has been used previously by other researchers for preparing carbon fibers to be measured by an AFM with successful results [36] [37] [38].

2.6 Overview of Atomic Force Microscopy (AFM) and PeakForce Quantitative Nanomechanical Measurement

2.6.1 AFM Overview

An AFM has been the instrument of choice to measure the transverse modulus of a single CF thread in the past [15] [16]. It is an instrument which is quite diverse in its applications and can be used for a myriad of different types of samples and purposes as it can gather several streams of data simultaneously. This machine has the ability to measure anything from resonating frequencies of a material, capacitance

of a circuit, to the amount of resistance a piece of material has to pinpoint pressure. It has been used in biology, electronics, and material analysis and has proven an excellent machine for several different research applications [39][40][41][42].

For an instrument that has many applications, the Peakforce mode that this project will utilize is rather simple in its operation. In general, the AFM relies on a cantilever that has a nm sized tip mounted on it. This tip moves across the surface and has three separate modes with which it can operate. It can be used in non-contact mode, contact mode, or tapping mode (Figure 3). Non-contact mode is mainly used for investigating electric, magnetic, or other atomic forces of a material by hovering over the material and oscillating the cantilever at or near the natural resonating frequencies of the sample. Contact mode is designed to measure attributes of the sample by maintaining contact with the sample's surface and gathering information on the interactions taking place. Finally, tapping mode, which will be used for this research project, involves a series of taps by the tip at programmed intervals and the subsequent deflection of the cantilever generates topographical data of the surface [43]. Furthermore, this data can be used in concert with the programmed settings to determine the amount of resistance a piece of material has to highly localized pressure [34].

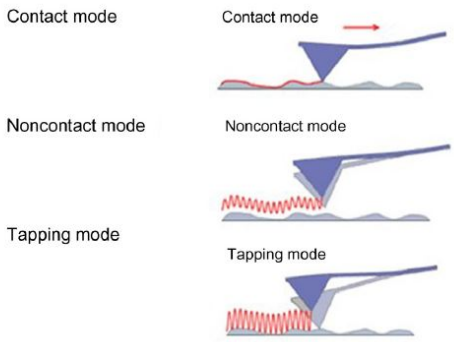

Figure 3. Depiction of the three modes of the AFM. Used with permission from Elsevier Books [39].

More specifically, the driving science behind how the non-contact mode of the AFM works is how the tip interacts with the surface via electrostatic forces, the way the positively and negatively charged atoms/molecules are attracted and repelled from each other. The Van Der Waals force also has an impact on the tip/surface interaction as it takes into account those weakly or not charged atoms/molecules and their attraction and repulsion to each other [44]. This is important because the AFM data is collected based on the deflection of the cantilever and how the tip is attracted or repelled from the surface of the sample has a direct impact on the data which the AFM collects. One research group went so far as to use these principles to link the wear of an AFM tip to the adhesion curve produced by the AFM [45]. As the tip wears down, the surface area of the tip increases leading to an increased attraction between the atoms/molecules of the tip and the sample surface. For this project's purposes, these attraction and repulsion forces generated by electrostatic, Van Der Waals, and even magnetic forces (due to the current from the laser) directly affect the deflection of the cantilever which is the source of the data [45] [41]. The cantilever is balanced on a spring as seen in Figure 4.

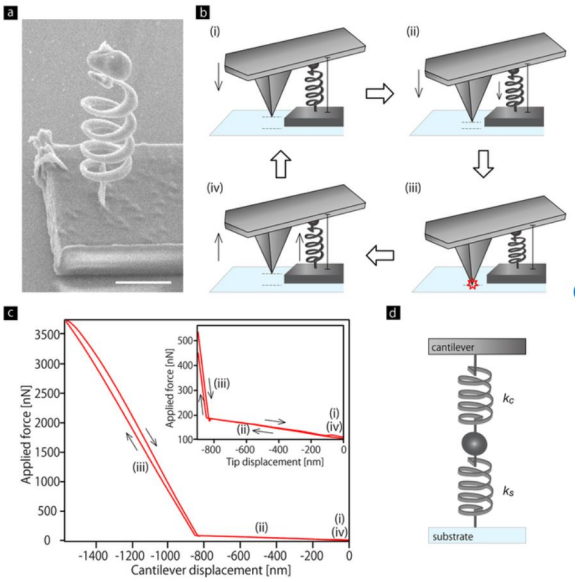

Figure 4. AFM spring interaction with the cantilever to produce data as observed with an SEM. Used with permission by Research Gate: Creative Commons [46].

With a known spring constant and a known deflection in the z-axis, the amount of resistance to the prescribed pressure imputed on the material can be accurately gauged. Raw data is great but having a visual representation of the data is always better. To that point the laser is the source for the deflection measurement which then can be converted and visualized as a heat map. The heat map is the translation of the different deflection heights into a visual depiction of the surface it is scanning, as seen in Figure 5. The image is not how the surface visually looks but rather the different heights of the material in question. Much like a topographical map, it detects the different deflection heights of the cantilever and displays them in an image. This image can be interpreted as different heights as indicated by the color scheme not an actual visual picture of the material [16].

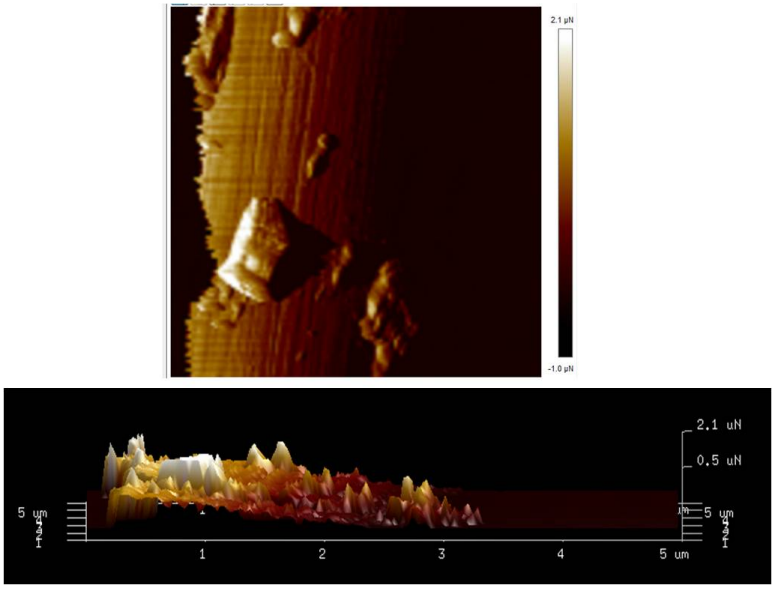

Figure 5. This is an example of a 2D and 3D AFM image.

2.6.2 AFM Data Collection

The type of data which the instrument produces is predominately gathered from force curves. Force curves, such as in Figure 6, show a graphical depiction of the tip movement and how much pressure is being applied as well as any adhesive forces present when the tip withdraws from the surface.

These force curves are than run through a proprietary algorithm to output discrete values associated with each data channel for each data point. The main data channel of interest in this research is the modulus data channel and the output is the reduced Young's modulus (in GPa) which is calculated by rearranging and fitting the Derjaguin, Muller, and Toropov (DMT) model to a force curve. To understand this better it is necessary to examine the DMT equation in the following section.

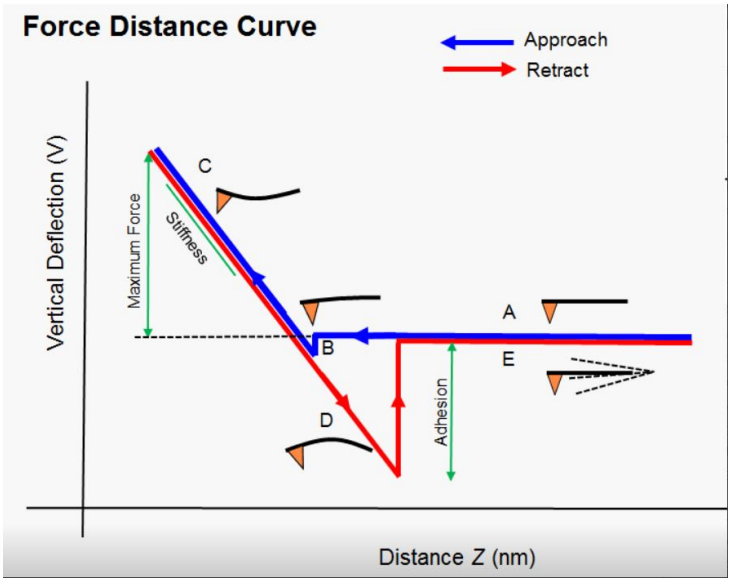

Figure 6. Depiction of a force distance curve created by the cantilever movement. Used with permission by Anton-Paar Instruments [47].

2.6.3 Modulus Theory

Young's Modulus, which expresses how well a material resists elastic deformation or its stiffness, can be depicted mathematically with the following equation:

$$E = \frac{\sigma}{\epsilon} \tag{1}$$

Where E is Young's modulus in units of Pascals, σ is the uni-axial stress/force in Pascals and ϵ is the unit-less proportional strain which is found by taking the change in length and dividing by the original length. In order to put this into terms that can be easily calculated using the AFM, the equation is adjusted to the following:

$$E = \frac{\sigma}{\epsilon} = \frac{F/A_0}{\Delta L/L_0} = \frac{FL_0}{\Delta LA_0} \tag{2}$$

where F is the force applied, L_0 is the sample thickness, A_0 is the indented surface

area, and ΔL is the indentation distance. Theoretically, this equation should be able to be used but it does not work practically due to the AFM tip being approximately 8 nanometers in diameter, making it essentially impossible to accurately know the indentation area with any degree of certainty. Though it is possible to collect all other values needed for this equation, the sample thickness, indentation distance, and the amount of force applied would be known as these variables would be input values. But without a good measurement for the indentation area it would be impossible to have have enough confidence in the calculations to make reproducible measurements.

As stated above, the Bruker AFM utilizes the Derjaguin, Muller, and Toporov (DMT) model which can be seen in Equation 3

$$F_e = \frac{4R^{1/2}E}{3(1-\nu^2)}\alpha^{3/2} = \frac{4E^*}{3}\sqrt{R\alpha^3} + F_a, \tag{3}$$

where F_e is the elastic repulsive force exerted on the surface of the sphere (or for the AFM the force exerted on the tip), R is the radius, E is the elastic modulus, ν is the Poisson's ratio, E^* represents the reduced Young's modulus, α is the depth of indentation, and F_a is the adhesion force. Furthermore, rearranging and solving for the reduced Young's modulus results in the following equation in which the repulsive force can be represented by

$$E^* = \frac{3(F_{tip} - F_{adhesion})(1-\nu^2)}{4\sqrt{R\alpha^3}}. \tag{4}$$

One thing to note, as highlighted by Frey, one of the main sources of uncertainty is associated with the AFM tip.[16] When calibrating the AFM there is a procedure for approximating the radius of the tip using a Bruker surface standard. This approximation is only accurate when the tip is first characterized since every time the tip comes in contact with a surface a little more of it is worn down. This means that it

is effectively impossible to have a perfectly characterized tip radius at any one time. Frey was able to quantify this error and developed a tip changing criteria to minimize its impact on modulus calculations [15] [16].

2.6.4 Practical Meaning of Young's Modulus

A ductile material will have a lower Young's modulus, the amount of resistance to elastic deformation, and a stiffer material will have a higher modulus. For example, a diamond has the highest known modulus as it is extremely resistant to elastic deformation. While glue would have a much lower modulus as it has little resistance to elastic deformation and is a lot less stiff. In this study of CF threads, any modulus that is measured which is significantly lower than the average is most likely measuring adhesive, sizing, or other contamination. The modulus of the CF thread will be much higher than any other material present and for that reason it will be important to focus on the measured modulus readings which are the greatest. Since the AFM will be applying the same amount of force it will be possible to compare the different moduli against each other.

2.6.5 AFM Tip

Because the area of indentation is required to calculate the modulus of the CF thread sample, it is important to be able to measure, as accurately as possible, the surface area of the instrument's tip. As depicted in Figure 7 the tip does not have a simple geometric shape but is actually formed by plane angles of 15, 25, and 17.5° +/- 2°. The specific tips which are to be used in this research are manufactured by Bruker and have a nominal equivalent radius of 8 nm. This nominal radius can fluctuate between 8 nm and 10 nm thus calibration of the tip size is required before measuring the sample for a more precise measurement. The AFM software has the

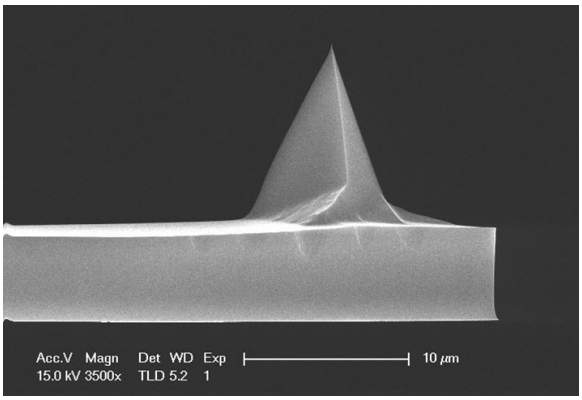

Figure 7. Image of a Bruker RTESPA-525 AFM Tip. Used with permission from Bruker Nano Surfaces and Metrology [?].

ability to characterize the tip shape and radius through the use of algorithms that reconstruct the tip based on its interaction with an instrument standard for a rough surface. Once the tip radius is attained via calibration that value must be input into the system by the user. This allows the instrument to calculate the reduced Young's modulus obtained from a sample based on the governing equations shown previously.

2.7 Statistical Operations

2.7.1 Distribution Skewness

When evaluating the data taken from the AFM, the easiest way to interpret it is to put it into histogram format where the X axis is the recorded modulus and the Y axis is how many times that particular modulus was recorded. Unfortunately, due to variables such as tip wear, height difference, potential contamination or defect on the CF thread there can be a wide distribution of moduli within a single scanned area. To easily extract meaning from data, a normal or Gaussian distribution would be ideal for statistical operations. Several researchers have used an AFM to evaluate the elastic modulus of various biological cells and natural polymeric gels and

have found the resulting distribution to fit a log-normal distribution [48]. However, a log-normal distribution is not ideal for using normal distribution based statistics and a right-tailed distribution (log-normal) makes precise data analysis difficult for this project. Furthermore, other research has been conducted on the tensile strength of materials, and it was concluded that for many materials the tensile strength, hardness, and fracture toughness are best represented by a normal distribution [49]. To ensure that the modulus distribution measured is close to a normal distribution a test needs to be conducted. A typical method to evaluate whether the moduli measured within a scanned area represents a normal distribution or not is to calculate the distribution's skewness. Since skewness is the measure of symmetry, this will indicate if normal statistics can reliably be used to evaluate and extract meaning from the measurement's modulus distribution. Standard deviation, mean, and mode are just three of the basic types of statistical analyses which would be rendered useless if the distribution was not close to normal. A common way to deal with distributions which may have a longer tail is to either take the square root of the values or the log of those values [50]. The following formula was used to evaluate the skewness of the CF thread's distribution:

$$Skewness = \frac{n \sum_{i=1}^{n} (x_i - \bar{x})^3}{(n-1)(n-2)s^3}, \tag{5}$$

where $\bar{x}$ is the mean, s is the standard deviation of the sample and n is the size of the sample set [51].

A perfectly Gaussian or normal distribution would have a skewness equal to 0, a slightly skewed distribution is between -0.5 and 0.5, a moderately skewed distribution is -1 to -0.5 and 0.5 to 1, and a very skewed distribution is anything below -1 or above 1. Standard statistics such as standard deviations are less reliable the more skewed the distribution. Figure 8 is a good comparison of one measurement's dis-

tribution compared to an ideal Gaussian distribution where a measurement refers to one area scanned compromised of 16k+ data points. It is important to check that the AFM moduli measurements fit a normal distribution otherwise all statistical information such as mean and standard deviation would not be accurate without additional statistical processes.

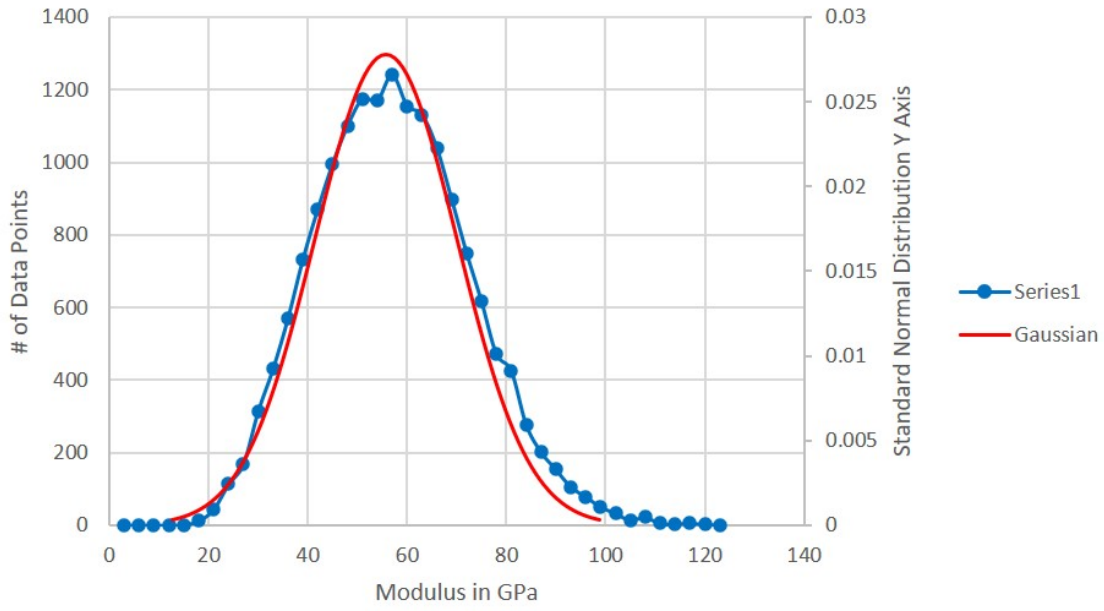

Figure 8. A comparison of a normal distribution to that of the measured moduli distribution collected from a 100 nm squared area of a single CF thread.

2.7.2 Theoretical Correlation Check

Whenever any instrument is used to calculate values it is always helpful to have a theoretical expectation to ensure the data obtained makes logical sense. For evaluating the modulus of a CF thread, theoretically, as the deformation depth increases the modulus should decrease as this indicates a less stiff material. Similarly, as the indentation height rises the modulus should also decrease. This is the theoretical way to check if the data collected is usable. Young's reduced modulus equation has several

variables which have an inverse relationship to each other like deformation height and modulus. Both of those variables have their own data channels in the AFM so a theoretical expectation check is possible. By rearranging Equation 3 so E^* is on the left side and F_tip (same as F_e) is on the right (see Equation 4) it is easy to identify these inverse relationships. In fact, the AFM can measure eight different data channels at one time, (Height, Modulus, Deformation, Indentation, PeakForce, PeakForce Error, Adhesion, and Dissipation). The easiest variables to evaluate in terms of impact on the theoretical modulus is deformation or indentation as this relationship should be linear as stated above. By evaluating the correlation between the deformation height and the modulus it will be possible to see if the AFM measurements make theoretical sense and will provide a scientific check on the validity of the method. If there is no relationship between the indentation, deformation, and modulus it would indicate there is an issue with the machine or algorithm it is using.

2.7.3 Analysis of Variance (ANOVA) Testing

An ANOVA test is the quickest way to see if there is a correlation between data channels that the AFM records. An ANOVA test is simply the comparison of two or more population's mean and if they are equal or not. From this information it is possible to find the P-value and see if there is a correlation between the two. The P-value is the statistical probability that an event will occur or in this case the probability that a change in the deformation height correlates to a change in the modulus. By performing an ANOVA test between the modulus, deformation, and indentation it will be possible to determine if there is a correlation between the modulus and any or all of the other data channels. If there is a correlation between the modulus, the deformation, and the indentation channels then it will confirm theoretical expectations. If there is no linear correlation between the deformation,

indentation and the modulus then it can be assumed there is an issue with the surface being measured, the AFM tip being used, or the instrument in general since the Young's modulus calculation is based in part on these factors. There may not be a 1:1 numerical correlation (the deformation height increases by 1.0 nm the modulus decreases by 1.0 GPa), but as the deformation height increases there should generally be a decrease in the modulus. It is important to remember a single measurement represents a scanned area that includes over 16,000+ data points so variance is to be expected. The ANOVA test will compare all the moduli recorded against the matching deformation height and a plot of the deformation height vs. modulus will quickly determine if a relationship exists.

III. Methodology

The methodology of this research project will be separated into two distinct areas. The first area is to prepare the CF thread for measurement by the AFM and the second area will be using the AFM to measure the transverse modulus of these CF threads.

3.1 Developing a Sample Preparation Method

A systematic methodology is required to mount micron-scale CF threads to a surface and prepare them for AFM analysis. A SEM stub was chosen as it provided a flat surface as well as being designed to be used in an SEM/FIB instrument. There are two primary reasons for critical failure in the sample mounting procedure. The first is not enough adhesive being present on the disk leading to the CF thread not being fully secured and the thread subsequently moving when in contact with the AFM tip. The second type of critical failure is too much adhesive being present and covering the CF threads resulting in the AFM collecting the adhesive's modulus data instead of CF's data.

The first critical error cannot be compensated for with mathematical modeling or statistical manipulation, as measurements will not be able to be taken in the first place. Adhesive covering the CF thread can be characterized by measuring the adhesive alone but it is not possible to simply subtract the modulus of the adhesive from the combined modulus of the adhesive and CF thread together. This is due to the fact the modulus which is measured will change with the the thickness of the adhesive/thread or contamination combinations. It is extremely unlikely the adhesive would have settled over the CF thread in a uniform manner, and even if it was uniform the procedure could not be reliably reproduced.

It must also be annotated that it is important for the CF threads to be adhered to the SEM stub surface as flatly as possible for precise results. Threads that have any degree of vertical angle due to the amount of adhesive below the sample may introduce additional uncertainty in the measured modulus. This is due to the fact that the CF thread does not experience the same transverse force from the AFM tip when it is applied at an angle vs. when it is applied perpendicularly. For each data point's Young's modulus (equation 4) to be comparable, the indentation area needs to be equal and if the thread is at an angle the indentation area will be influenced. A great visual reference would be to think of hitting a wooden board with a hammer. If that board is flat the indentation from the hammer head will have a generally consistent depth all the way around. If that same wooden board is laid down on an angle and hit with the hammer (using the same force) the indentation depth from the resulting blow would be uneven. The same effect applies to the AFM tip making contact with the CF thread. If the deformation depth is inconsistent than the transverse modulus which is derived, in part, from this variable would also be inconsistent. Though the small scan area size will reduce the uncertainty due to any slope of the CF thread, theoretically it would still be minimally present if the thread is not flat. Since the modulus being measured for this project is relative, minimizing any kind of slope is ideal. Threads which are stacked on top of other threads or a large quantity of epoxy (greater than 2 µm) will be avoided.

3.1.1 Thread Separation Approach

In order to mount the individual threads a CF thread must first be extracted from the tow of CF. One method to do this is to cut a section from the tow and then use blunt force to separate out the individual CF threads [16]. The method which was ultimately the most successful was to hold down a 1 mm or less length section of CF

tow onto a glass slide with one tweezers and use another tweezers to pull individual threads from the anchored section of tow. This process was repeated until the entire 1 mm section of tow had been reduced to its individual threads. To be able to see the individual threads during this separation process a table mounted 3x magnifying glass was used. It should also be noted that during the process the CF threads would also break apart yielding sections of CF thread that were micron sized.

One issue which arose was the presence of static electricity on the individual threads. Each thread would 'jump' and cling to a group of other threads making separation difficult. It was hypothesized that introducing moisture to the process may reduce the static electrical attraction between the threads. A drop of water from a pipette was placed onto the glass slide and the CF tow section was submerged and separated while in contact with the water making it dramatically easier to separate the CF threads from the tow. Once the threads were separated the sample was allowed to dry until all the water had evaporated, leaving behind the separated threads on the slide. These threads were then easily picked up and/or brushed onto an adhesive covered SEM disk for further observation and preparation work.

3.1.2 Sample Preparation for AFM

In order for the AFM cantilever to produce accurate data several variables need to be addressed and minimized with sample preparation. For the CF threads in this project it is important that the thread is affixed to the SEM stub surface and cannot move when the tip of the AFM is in contact with it. Any rolling of the fiber would cause issues from data collection continuity to the destruction of the tip due to hitting the sample substrate instead of the sample itself. Previous research has shown that the CF thread can be affixed to a small aluminum disk using various forms of superglue with adequate results.[16] The difficulty lies in ensuring the glue does not

cover the fiber as it cures. This method of affixing the sample using an epoxy or glue seems to be the consensus within the community; however, to do so without covering the sample is more of an art than a science and will be discussed in Section 3.1.4 [15][52][21].

3.1.3 Adhesive Selection

At the beginning of this research project the FIB/SEM instrument was not available and the previous method for mounting samples with superglue was attempted [16]. Issues with the superglue included it drying too fast to create an evenly applied layer over the aluminum disk. The resulting unevenness and general roughness of the superglue exacerbated horizontal tip crashes, a crash that results from the tip moving horizontally and running into an adhesive peak. The superglue being translucent also made it impossible to tell if the superglue covered the thread even when using a powerful Keyence 3D microscope at a 6000x zoom.

Alternative methods were attempted such as trying to use nail polish instead of superglue. The primary reason behind attempting nail polish was the ability to have a color contrast between the thread and the adhesive. If there was color contrast then any thread covered with the nail polish could easily be visually identified. It was also reasoned that nail polish had enough adhesive properties to render the CF threads immobile. However, this adhesive experiment was abandoned when the SEM/FIB instrument became available because the off gassing properties of the nail polish were unknown and placing it in the vacuum chamber of the SEM/FIB was deemed too risky. It was decided to use a two-part epoxy (JB Weld, Clear Weld-2Part Epoxy) instead of superglue or nail polish as an adhesive. This particular two-part epoxy had already been used with the SEM/FIB instrument and had been authorized for use. In a happy coincidence the two-part epoxy was also found to be softer than superglue

when it cured, resulting in a reduced number of horizontal tip crashes.

3.1.4 Application of Adhesive

To adhere the CF threads, a small amount of epoxy was put onto the SEM disk and spread minimally across the top using a cotton tip. However, this was problematic as it did not spread evenly and created a plethora of peaks and valleys in the epoxy from the individual cotton threads dragging unevenly across the surface. The back edge of a scalpel was then used with better success as it was able to evenly coat the SEM disk with a thin layer of epoxy. Once the epoxy was evenly spread on the SEM disk, the separated threads were placed or brushed on top of the epoxy using a tweezer.

Previous research conducted by Frey and Veigas also used a similar approach for mounting samples with one major difference [15][16]. Once the threads had been mounted to the disk, acetone was applied at regular time intervals to attempt to remove any excess superglue from the top of the threads. This was due in part because Frey and Veigas only had a 3x magnifying glass to observe the samples and many of the CF threads were assumed to have excess superglue covering them. To combat this issue, the threads were treated with acetone to attempt to remove as much excess superglue as possible. With the introduction of the SEM/FIB instrument to the preparation method the application of acetone became unnecessary. The threads could now be observed in an SEM to determine if they were covered with adhesive. Epoxy experiences a charging effect when bombarded with the electrons generated by the SEM whereas the CF thread material does not. This contrast made it possible to determine if a thread was covered or not covered by the adhesive. If a section was slightly covered the FIB was used to ablate the adhesive away and is discussed in Section 3.1.6

3.1.5 FIB Power Selection

Before discussing how the FIB rastering process was accomplished, the method for the FIB power selection must first be addressed. The Tescan FIB/SEM instrument (Model: Lyra 3 GMH (FIB)) had many different power output options which ranged from 92pA to 6.49nA. For practical purposes more power equated to more material being removed for the same time duration applied. When beginning the power selection process the lowest power setting was chosen (92pA) but the rate of ablation was too slow and it was hard to tell when to stop ablating the CF thread. The method developed which determined when to stop ablating a CF thread will be discussed in greater detail in the next section but for the purposes of this section, 92pA was too little power. The power was then increased to the highest setting (6.49nA) but in this case the thread was ablated too quickly. By the time a CF thread was located and spot selected on the thread for ablation too much material had already been removed. It was decided the best way to evaluate the correct amount of power to use was to start with the lowest power setting, evaluate how fast the FIB ablated away the material, and if it was too gradual, adjust the power to a higher setting. The goal was to find a power setting which would ablate away the required amount of material at a rate where the ablation of the contamination on the thread could be observed and controlled. Stepping through each of the discreet power selections from the lowest it was determined that applying 273pA of power was sufficient to ablate any contamination while still maintaining control of the process. Any more power created issues with ablating the CF thread too quickly.

Power selection for just ablating the excess epoxy/contamination was just the first portion of the power selection process. The other power selection process was what power to use for cutting through the CF threads. There was no reason to spend more time than what was necessary to create an effective cut in the CF thread so a higher

power was most ideal. However, to avoid destroying the thread while looking for a suitable place to cut, the lowest power setting was used to locate before the power was adjusted to a higher power setting (3.6nA) to perform the cut. This process of switching between rastering and cutting will be discussed more in detail in Section 3.1.7.

3.1.6 Using the SEM/FIB to Locate and Raster CF Threads

To observe the CF thread and complete the preparation of the thread before collecting modulus data with the AFM a combination FIB/SEM machine was used. An SEM is much better at observing objects and less destructive due to using electrons instead of ions so a combined system of SEM and FIB is not uncommon to find. The combination of an SEM and FIB make locating and ablating/cutting an object much easier, as an object can be cut/ablated by the FIB and then immediately viewed with a click of a button to see the result with greater clarity with the SEM. Prior to moving the CF threads that had been adhered to the SEM stub to the FIB/SEM instrument, the epoxy was allowed to cure for a minimum of 12 hours. The regular procedure would be to use a low magnification to see the entire SEM stub surface first and then focus on likely areas which had exposed, or uncovered, CF threads present. Though a prepared SEM stub with CF threads adhered to it may have appeared to have the majority of the threads uncovered, when viewed with the naked eye or the 3x magnifying glass, most of the threads were actually covered when observed with an SEM. Each prepared sample of CF threads always did have some uncovered, it would just take varying amounts of time to locate them. One technique which was developed was to begin observing around the edges of the SEM stub and then move towards the center since the majority of uncovered threads were initially found on the edge. Once a section was found, the platform inside the machine was tilted from

a 90 degree angle with respect to the SEM to a 55 degree angle. This was required so the FIB would then be positioned at a 90 degree angle to the CF thread. Figure 9 is a photo taken inside the vacuum chamber to better illustrate the different angles the platform needed to be adjusted to in order to most effectively use the FIB and SEM.

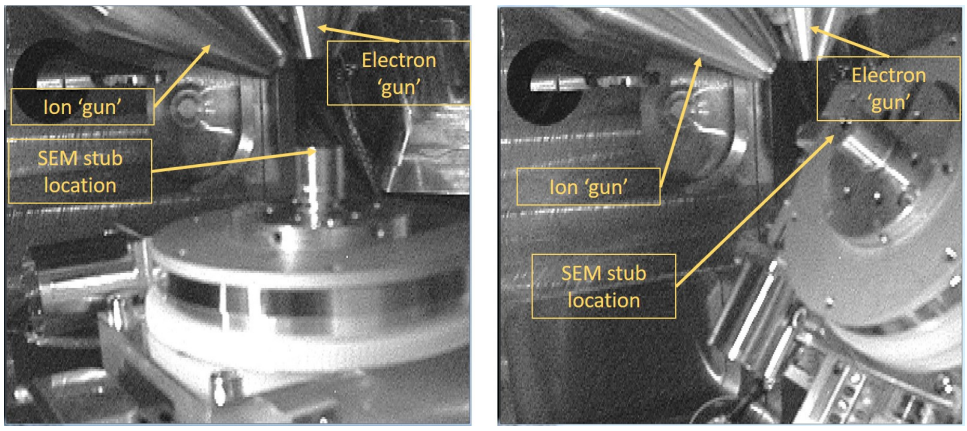

Figure 9. (left) Sample platform shown at a 90 degree angle with relation to the SEM, this is the way the CF thread samples are loaded into the instrument and initially observed. (right) Sample platform shown at a 55 degree tilt with respect to the SEM and a 90 degree tilt with respect to the FIB. This is how the CF threads were rastered with the FIB.

Once the platform was in position and the working distance adjusted to 9nm the FIB was turned on using a power of 127pA. As discussed in the previous section this was to minimize any ablation of the CF thread and adhesive while locating and syncing the SEM and FIB views. The FIB view was then synced with the SEM view so both apertures were focused on the same point. This was required as the SEM gives a much clearer view of the surface that is being ablated compared to the FIB. The SEM also was now viewing the thread at a 55 degree angle so it was easy to tell if too much material had been ablated. When properly synced it only required one command to turn off the FIB and turn on the SEM to view the focused area. Once the CF thread of interest was located then the power of the FIB was adjusted to 273pA and the surface of the CF thread was rastered for an average of 60 seconds

until all visible gross contamination on the thread was removed.

Similar to viewing epoxy with the SEM, the epoxy also has a charging effect when observed by the FIB, making the adhesive easy to identify. Rastering is just the term used when the FIB is bombarding the surface with positive gallium ions to show the contrast/image of the sample, not actually performing a cut or focused ablation of an object. So when the FIB is being operated just to view an object/sample it is actually continually rastering for the duration the FIB is powered on. This is the same as when an SEM is viewing an object, but an SEM uses electrons which is mostly non-destructive and does not ablate any material. When rastering the CF thread, the technique which was used was to ablate away the epoxy until the charging effect slowly faded and the CF thread became a dull or black colored image as is seen Figure 10 that indicated the majority of contamination had been cleared. This process took on average about 60 seconds. The SEM view of the same thread can also be seen in Figure 11.

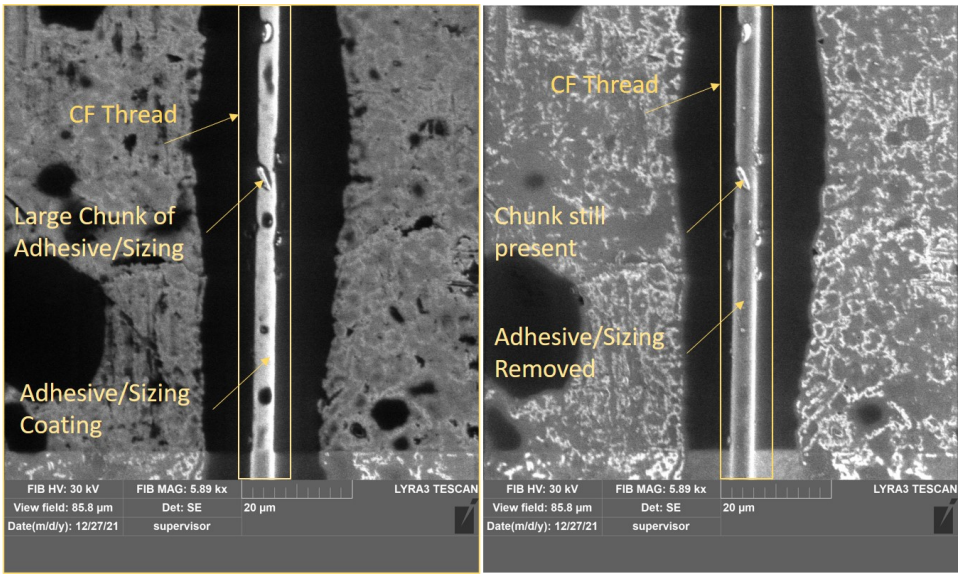

Figure 10. A Pre (left) and post (right) FIB photo: Adhesive/Sizing experiences a charging effect when exposed to the FIB and the image of the CF becomes dull after the majority has been ablated away.

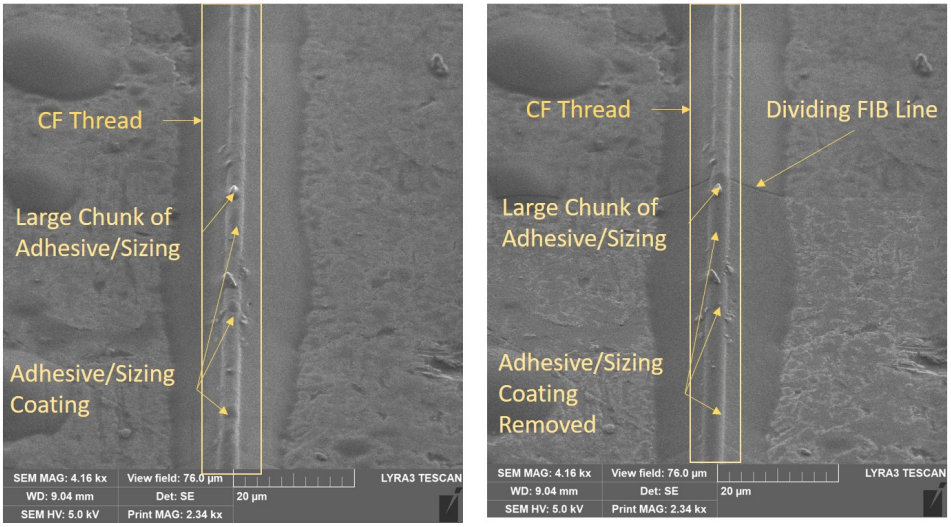

Figure 11. A Pre (left) and post (right) FIB photo taken by an SEM: The ablation of the epoxy and sizing from the CF thread is visible.

Both the before and after images still retain relatively large chunks of debris, the exact chemical makeup of those chunks cannot be determined with the instruments used in this research but their presence actually helps to identify a specific location on the CF thread to be measured by the AFM. Figure 12 shows the same section of fiber but viewed under the Keyence microscope at 6000x magnification. The particular Keyence microscope used was a VHX-7000 model which is a digital 3D microscope which can capture high resolution images, making it ideal for recording the locations of specific CF threads. It is clearly evident that the section shown in Figure 12 has been cleared of the majority of adhesive/sizing and other debris. Though it is impossible to say that absolutely all of the contamination of the thread has been removed, it is possible to conclude that the majority has been removed. Since this research project is dealing in relative measurements and not absolute measurements, this is acceptable.

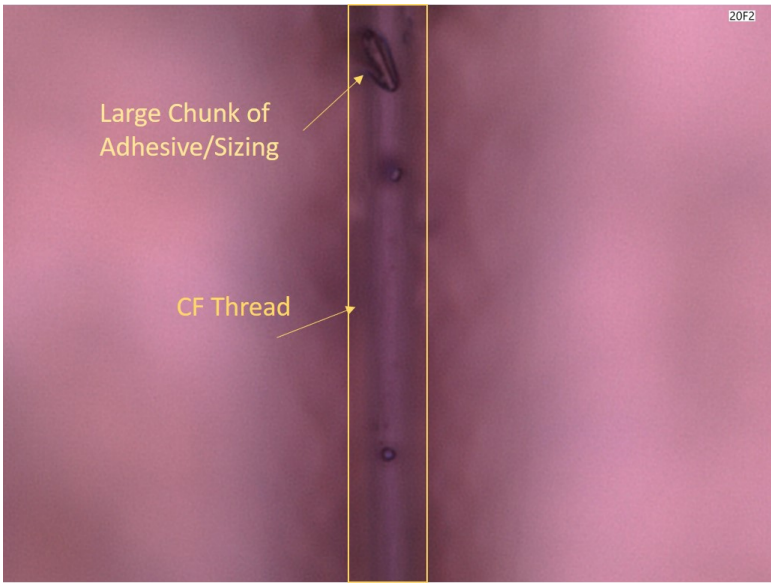

Figure 12. This is a photo of a CF thread under an optical microscope at 6000x magnification after it has been exposed to a FIB.

3.1.7 Using the FIB to Cut CF Threads

Not only was the FIB used for rastering sections of CF threads but in the majority of instances it was necessary to use the FIB to cut the CF thread down to a certain length. To accomplish this, the FIB was tuned to a higher power output of approximately 3.1 nA, and focused down to an approximate 20 nm wide section of thread for four minutes. Once the time had expired the cut was observed with the SEM to ensure the thread had been cleaved completely. Figure 13 is an example of what a thread looks like once cut by the FIB. The FIB software does have a function which allows the user to choose a material/element from a library, power setting, and depth to ablate (in microns); and the software will predict the time required to ablate that much material. However, the library does not contain CF but it did have the element carbon, which was selected. A depth of 5 µm was entered and as was stated earlier a power setting of 3.1 nA was chosen. Because a CF thread is chemically different than elemental carbon the time predicted by the software was never enough. To work around the software limitations instead of choosing an ablation depth of 5 µm it was doubled to 10um and checked after four minutes. If the thread had still not been cut then the FIB was again turned on and checked every 45 seconds until the thread was cleaved.

3.2 Methods Attempted but Discarded

3.2.1 Using a Material Grinder to Prepare Samples

Prior to using the SEM/FIB for the first time it was thought that some adhesive may need to be ground off the SEM disk. This method was only attempted once and when compared to CF threads which had not had any adhesive ground off it was apparent the grinding did much more structural harm to the mounted threads

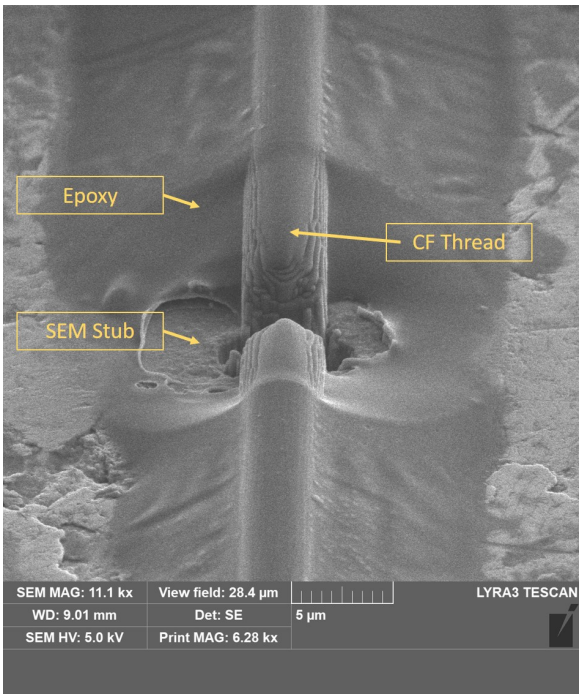

Figure 13. This is a photo of a CF thread after being cut with the FIB.

than benefit. The threads, if coated, were so lightly coated that any grinding immediately cut through the epoxy and either obliterated the CF threads or severely damaged them. As stated above, it was evident that the grinding was unnecessary after observing the threads in the SEM/FIB; and the method was discarded.

3.2.2 Uncovering CF Threads with a FIB

Another method that was attempted involved trying to ablate epoxy from a CF thread which had been completely covered, with little success. The epoxy would be reduced by the ion beam but it was impossible to gauge the correct time and intensity needed to clear a carbon fiber thread due to the varying thickness of the epoxy covering the thread. Most often, the FIB would ablate all of the epoxy and then parts of the CF thread; other times, it would only ablate a portion of the epoxy

without exposing the CF thread. There was no way to gauge how long or what power intensity was optimal to only ablate the epoxy and not the CF thread due to the variations in the epoxy thickness. After multiple attempts it was determined that finding an uncovered section of fiber was much more efficient than trying to uncover threads that had been encased in epoxy. However, in the event all threads were covered on a prepared SEM stub uncovering a thread is possible; it just requires a painstaking amount of time and patience. This is because every 15-30 seconds the thread has to be checked to ensure the thread has not been damaged by too much ablation.

3.3 CF Thread Analysis Method Overview

Once the CF thread's were rastered and/or cut by the FIB the SEM stub with the prepared threads was transferred to the Keyence 3D microscope. The stubs were placed in a 14 count SEM stub holder where they would remain for the duration of the experiment. The SEM stub holder was then oriented with the number 1 stub location at the 12 o'clock position and the stubs themselves were adjusted so the threads which had been exposed to the FIB were aligned from the 6 to 12 o'clock position. Images were then taken to record the location of each thread on the SEM stub before the SEM stub with the threads were transferred to the Bruker Icon Atomic Force Microscope. This particular AFM is mounted in an atmosphere controlled box where the oxygen and water content was maintained at less than 0.1 ppm; the pressure was also controlled and remained at 4.7 mbar. To ensure the modulus measurements were reproducible, the AFM was calibrated and tip characterized before each data collection session.

3.3.1 AFM Cantilever and Tip Calibration

The Bruker technical manual for the NanoScope 1.4 software was followed to ensure the cantilever was calibrated and the tip was characterized correctly and to specifications. The only difference pertained to the Bruker tip characterization method. For this research experiment instead of using the prescribed scan size of 1.5 µm with a ratio of 1, a 5 µm scan sized was used with a ratio of 4. The ratio of 1 means that the horizontal distance measured to vertical distance measured is a 1:1 ratio. A ratio of 4 simply means the horizontal to vertical distance measure is 4:1. This change in scan size and ratio had been used previously with this instrument, and it has been noted the different size and ratio provided a more successful tip characterization [15]. The tips used for this experiment were the Bruker RTESPA-525 as previous studies found these tips to give the best results [16].

3.3.2 Locating the Ablated CF Thread with the AFM

Before removing the SEM stubs from the SEM/FIB instrument, an image was taken with the SEM prior to the SEM stubs with the prepared threads being transferred to the Keyence 3D microscope. The stubs were placed in one of the 14 count SEM stub holder (puck) positions where they would remain for the duration of the experiment. Since the epoxy was clear and the ablated threads cannot be distinguished until the magnification is increased, if the general area and shape is not known then the ablated areas are impossible to find using just the AFM's optical microscope. What quadrant the ablated thread was located was recorded prior to removing the threads from the SEM/FIB instrument and the thread was once again located with the digital microscope to photograph. This photo would enable the ablated thread be located as it would show the orientation of the ablated thread and the surrounding unablated threads in much the same way as it would be viewed using the AFM's op-

tical microscope. The reason why the first photo taken by the SEM could not be used for this purpose is because the image looks completely different than what would be viewed using the AFM optics, a more similar photo was required. The AFM's optical microscope used to locate threads to be measured does not have a high resolution nor wide field of view making it hard to locate threads if the general area is not known. The final indication that a thread had been exposed to the FIB was the presence of rectangular 'burn' marks surrounding the thread where the FIB had ablated the epoxy on either side of the thread. Figure 14 is an example of an image taken with the digital microscope to pinpoint an exact location of a particular thread to compare with the AFM view as seen in Figure 15.

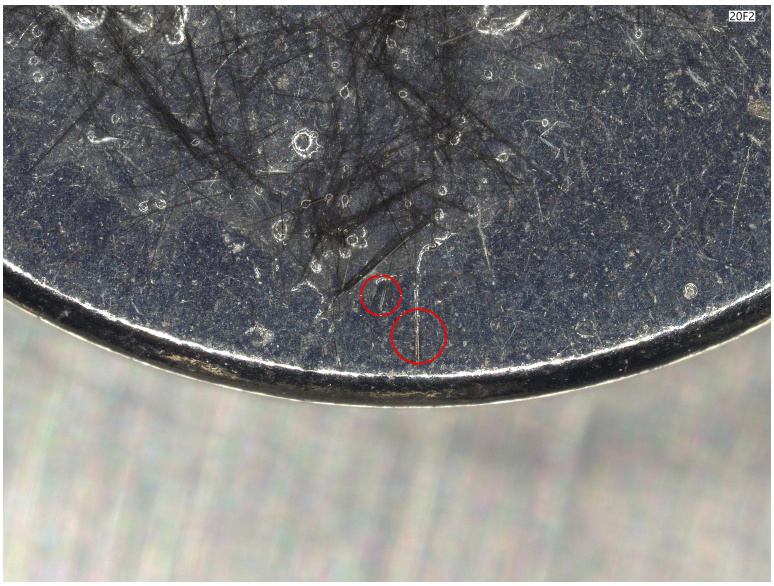

Figure 14. This is a 3D microscope image of the two locations which were exposed to the FIB.

It was also crucial to position the SEM disks with the same approximate alignment as they were viewed under the 3D microscope. If this was not done then knowing what quadrant the location of the thread resided was pointless. This was accomplished by ensuring the SEM stub holder always had the number 1 sample position (as labeled

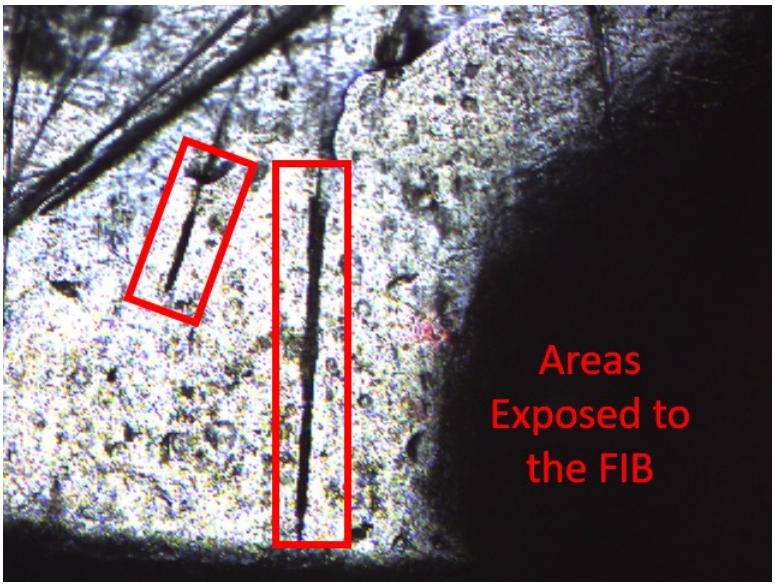

Figure 15. This is a photo depicting both thread locations that were exposed to the FIB and the telltale rectangular burn marks which make the thread appear wider.

on the puck) pointed at the twelve o'clock position. Additionally, when locating the threads with the Keyence 3D microscope, each SEM stub was rotated until the ablated thread was positioned so that it ran vertically from the six to twelve o'clock position. This alignment was found to be the easiest alignment for the AFM to locate since the tip moved horizontally and provided the best chance for detecting any height difference which indicated the thread's presence. When developing this method there were several times when taking photos with the 3D microscope was skipped because the location was thought to be obvious. But after searching for over half an hour with the AFM optical microscope, the step would inevitably have to be completed because it was impossible to compare the SEM photo to what was being seen by the AFM.

Once the ablated CF thread had been located, finding the specific area on that thread which had been rastered was the next step. It was observed that the CF thread when exposed to an ion beam looks lighter in color compared to the rest of the thread

that was not exposed to the ion beam as shown in Figure 16. It would be ideal to

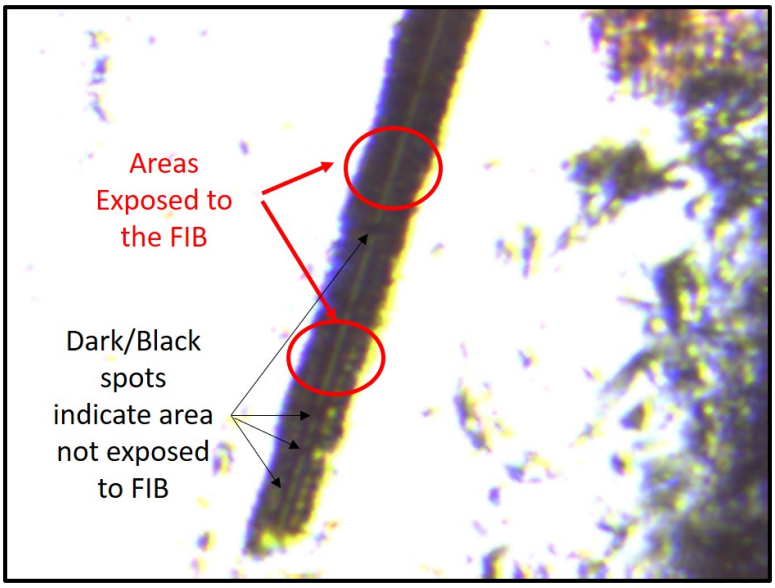

Figure 16. This is a photo of 2 Locations on a CF thread which were exposed to the FIB.

locate the previously identified spot along the length of CF thread that was observed by the SEM and Keyence microscope to be 100% that the section being measured with the AFM was ablated but that was not always possible or practical. The formation of debris which was identified previously is an approximate 5 µm section of a 200 µm length CF thread that had been exposed to a FIB. Since each 5 µm section takes a minimum 15 minutes to measure, it was not efficient to find the exact spot. Instead of hunting for the exact spot on the thread, the AFM tip would instead be placed in the center of one of the 'lighter' sections that is seen in Figure 16. This method was developed out of necessity after spending many days trying to find the exact spot which was photographed with the SEM and 3D Microscope.

To further confirm that the AFM was indeed measuring a location which had been exposed to the ion beam, the PeakForce data channel image (map) was utilized. This data channel essentially produces a map of the surface using the peak force

measured during the scan. Any portion of the fiber that was mostly cleared of any adhesive/epoxy and other debris was suitable; it did not have to be the exact section of thread that was previously observed. Since the area that was measured and recorded by the AFM was at most 1 µm^2 compared to the 200 µm length of the CF thread that had been exposed to the FIB there was plenty of CF thread that had been ablated. It was just important to measure a section which did not have any gross contamination present. Throughout this study, there were times when the AFM was accidentally measuring a section that had not been ablated; and the difference was visually apparent as a thread which had been ablated had a non-homogeneous surface.

The main reason for trying to find the same area that was captured by the SEM and Keyence microscope was in line with the old adage aim small, miss small. Instead of just looking for any rastered section on a thread, if a specific portion of that exposed thread could be targeted, then the chances of accidentally measuring a section that had not been rastered decreased. The AFM has cross-hairs present on the view screen where the tip theoretically should be located. However, it is not uncommon to be off by two or three microns in either the X or Y direction due to variation on how each tip is set. To ensure the tip was actually in contact with the CF thread, a search pattern had to be developed. The scan size was set to 5 µm and the height data channel was observed in real time as the tip scanned. After four or five horizontal passes if the height of the surface measured did not change (or changed only by 5nm) then the thread had not been located. The tip would be offset to the right or the left based on a visual observation and another 5 µm scan was initiated. This procedure was repeated until the height data channel displayed a curve with a height from 500 nm to 1.5 µm. Once this curve was identified then the entire scan was allowed to complete in order to locate a suitable portion of the thread to focus further.

Figure 19 was a typical PeakForce image of an area that was exposed to the FIB,

from here the instrument was focused on a particular area that did not have any gross imperfections present as indicated with dotted box.

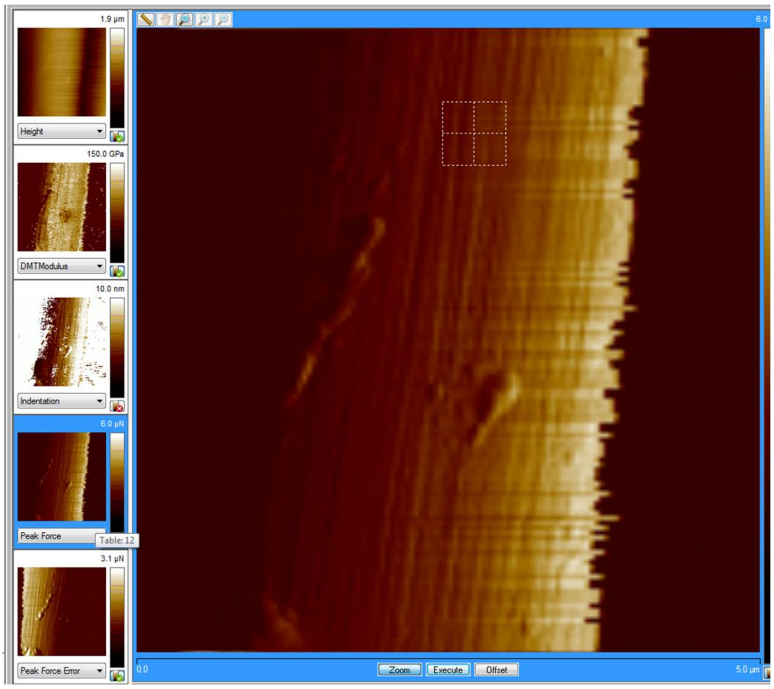

Figure 17. This is an example of an AFM image used to locate suitable sections of the carbon fiber thread for measurement, the suitable area has been annotated with the dotted box.

3.3.3 Tip Exchange Criteria

In order to ensure precise modulus measurements it was crucial to have a tip exchange criteria. Frey used a tip criteria of either ten measurements of the same CF thread or every time a new CF thread was measured. Because the two part epoxy did not wear the tip away as quickly, this project chose to limit the total number of measurements at 15. This was decided after checking the tip radius every 10 measurements for a week, and the tip was not being worn down as quickly as was seen in previous work [16]. Other factors which would result in a tip exchange were as follows: anomalies in the real time-force curve display, consecutive measurements

that had extreme variations in the distribution, or 15 measurements had been taken with the same tip. If the machine had been sitting for more than 12 hours but did not meet any of the tip exchange criteria, then the tip would be re-calibrated but not changed unless the tip radius was characterized to be over 20 nm.

3.3.4 AFM Interface

This research project only adjusted a couple of variables on the AFM interface and Figure 18 outlines what adjustments were made from the default settings on the AFM Bruker NanoScope 1.4 and the reasoning behind the adjustments.

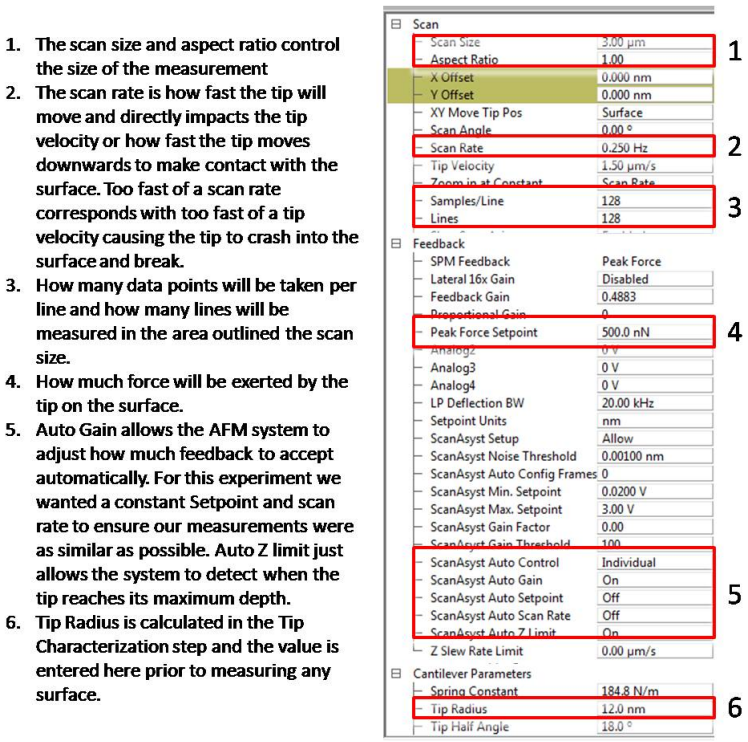

Figure 18. This is an example of an AFM interface, the highlighted areas are the parameters which were adjusted in this research project.

One caveat to item 2 in Figure 18 is that the scan rate was initially set at 0.5 Hz but after many tip crashes it was adjusted down to 0.1 Hz. The tip velocity automatically adjusts based on the scan size and it was approximately 0.005 µm/s for a 100 nm scan

size. Every measurement took approximately 35 minutes to complete and as more data was required, it was decided a 0.25 Hz scan size was adequately slow enough to not damage the tip and still extract data. If time was not an issue it would have been ideal to do every scan at 0.1 Hz simply because the standard deviation for the average modulus was lower by 2-5 GPa meaning the data had less variance.

3.3.5 Locating An Ideal Section to Measure with the AFM

As described earlier, the procedure of measuring using the AFM was to set the scan area to 5 µm to ensure that the thread had been located before focusing on an area 1 μm^2 or less. Looking at Figure 19, the thread is clearly visible, as are the portions on the thread which still have adhesive/sizing or other contamination present. Once the

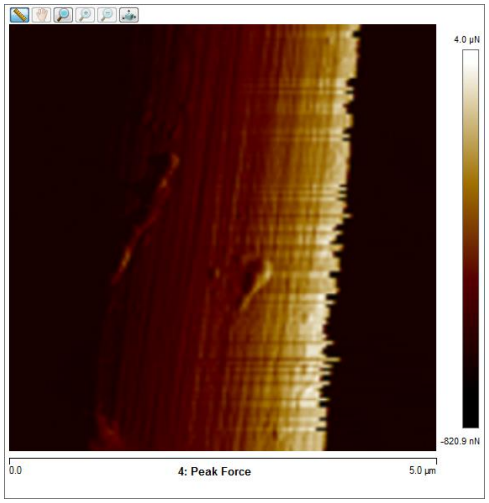

Figure 19. This is a 5 μm^2 area PeakForce data channel window example from the AFM.

thread was located, the AFM modulus window was utilized to pinpoint the area with the highest modulus as is shown in Figure 20. (The lighter the color the higher the modulus, the darker the color the lower the modulus). Once the area with the highest modulus was located, it was then checked against the indentation and adhesion data channels to ensure both values were acceptable. Acceptable here equated to no more

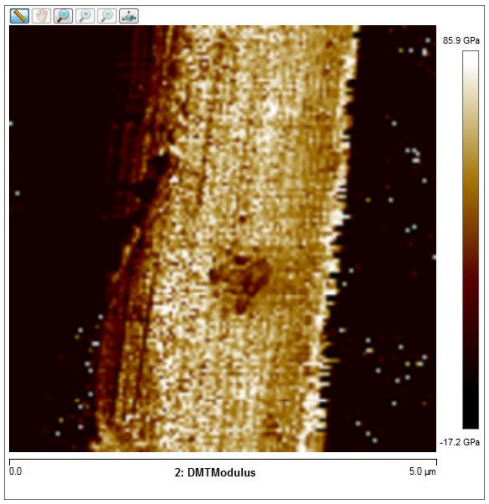

Figure 20. This is a 5 µm^2 area modulus data channel window example from the AFM.

than 5 nm indentation depth and roughly 0.0 nN for adhesion forces as is seen in Figure 21 and Figure 22. If all data channels indicated the focus area to be measured

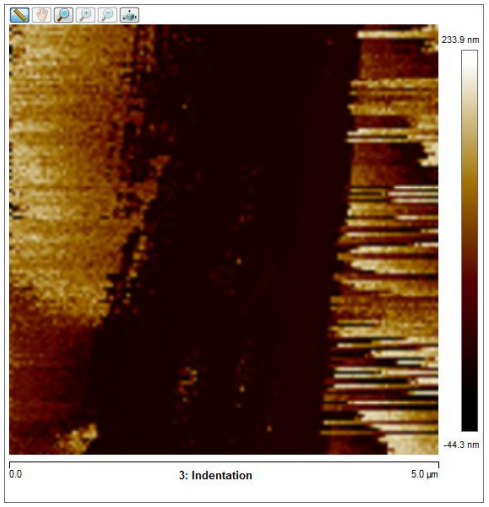

Figure 21. This is a 5 µm^2 area indentation data channel window example from the AFM.

would be acceptable, the AFM was engaged and the measurement was taken. The AFM was set to take 128 samples per line for 128 lines which equates to 16,386 individual data points per single AFM measurement. Once the measurements were

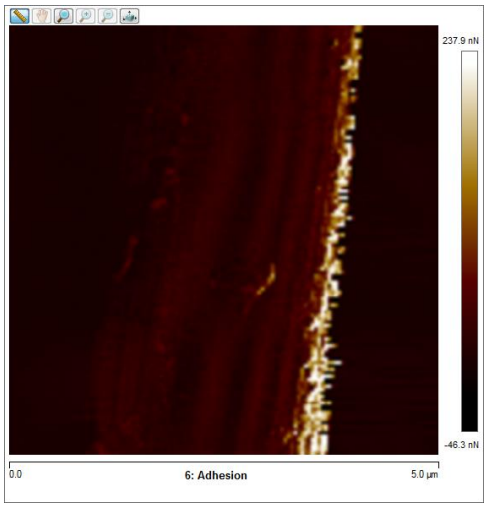

Figure 22. This is a 5 µm^2 area adhesion data channel window example from the AFM.

complete then the location was offset by 100 nm and another measurement was taken. The goal was to measure a total area between 500 nm and 1 µm squared. This procedure of locating and pinpointing specific areas on an ideal section of thread was repeated a minimum of 3 times. For each CF model number a minimum of two threads were tested, one being less than 200 µm in length and the other being greater than 500 µm in length. This was to ensure that the overall length of the CF thread being tested had no influence on the measured modulus.

IV. Results and Analysis

4.1 Overview

The sample preparation method can be broken into three distinct areas: carbon fiber thread separation, mounting carbon fiber threads, and carbon fiber thread cleaning. Five PAN CF threads were measured after they were prepared with the developed method; and the data was analysed using probability distributions, ANOVA testing, and graphical representation. One of the CF threads was an export-controlled thread of unspecified origin that was compared to the others to evaluate if there was any significant difference between it and the commercially available CF threads. This chapter will first cover the results and analysis of the new CF thread preparation method followed by the results and analysis of the measured moduli recorded. The last thing which will be discussed is how the commercially available CF threads compared to the export-controlled CF thread and any insights observed. It must be noted here in the introduction for clarity that a measurement refers to one scanned area comprised of 128 lines and 128 points on each line equaling 16,384 data points of which there are eight different data channels. These data channels are height, modulus, indentation, adhesion, Peakforce, Peakforce error, dissipation, and deformation. This means each measurement has over 131,072 individual values associated with it.

4.2 CF Thread Sample Preparation

4.2.1 Carbon Fiber Thread Separation

Using water to reduce the static electricity of the CF threads greatly improved the separation process. Before introducing moisture to the separation process the threads were nearly impossible to separate. Adding moisture, the amount of time it took to separate the threads was improved by nearly 50%. This was measured by timing how

long it took to separate the fibers without the water and then once the water was used as well as the amount of threads which were able to be separated. Without any moisture, the process of separating the CF threads took approximately 15 minutes for a 1 mm length tow and not all of the tow could be completely separated. By introducing moisture to the process the same length tow could be separated in 6-8 minutes and the entire tow could be reduced to individual threads.

4.2.2 Adhering CF Threads with Epoxy vs. Superglue

Using a two-part epoxy was necessary to limit off-gassing while in the vacuum chamber of the FIB/SEM but after mounting over 20 samples other additional benefits became evident. The epoxy required a longer time to solidify and cure, making it much easier to evenly spread across the SEM stub. This in turn contributed to less AFM tips being broken as the quantity of adhesive valleys and peaks was reduced. When measuring CF threads that were adhered with superglue, more than 14 tips were broken just attempting to locate the CF thread to perform measurements. This not only was expensive, but also equated to lost time. Every broken tip had to be changed immediately and the AFM had to be re-calibrated, all of which would take a minimum of 30 minutes if everything worked the first time. The number of tips that were saved made the switch to the two-part epoxy worth it. The total number of tips broken once the two-part epoxy was used was reduced to two.

4.2.3 Ablating CF Threads with a FIB

This project introduced the use of a FIB to ablate sizing and/or other contaminants from the surface of a carbon fiber thread. Initially, an attempt was made to use the FIB to cut down to the center of a CF thread, but after repeated attempts, it was realized that the damage sustained by the thread during this process was too

extensive. The time and energy required by the ion beam to cut down to the center of a CF thread resulted in a thread that no longer retained its original shape or form, but rather looked like a melted candle. Subsequently, the FIB was used at minimal power to raster the surface to ablate gross contamination and sizing off of the thread without penetrating any further. This enabled the AFM to measure the modulus of the CF thread without a coating of adhesive or sizing to influence the modulus data collection. It cannot be stated that all adhesive and/or sizing was removed, but enough was removed that the fiber shape and structure was easily seen. By reducing the amount of contamination on the fiber, the modulus values measured were on average 58% higher than modulus values measured without the use of a FIB. This was determined by comparing values of the modulus collected from areas that had not been exposed to the FIB to those values obtained from areas which had been exposed to the FIB. Table 1 are six representative comparison measurements from a single thread (Model: AS4GP12K). These six measurements were taken with a single tip to preserve the continuity of the data.

Table 1. Comparing the effect on the modulus when a thread is exposed to a FIB and when it has not been exposed to a FIB.

Type of Section Measured	#1 (GPa)	#2 (GPa)	#3 (GPa)
Measured section not exposed to a FIB ±3.6 GPa	25.91	27.58	31.70
Measured section exposed to a FIB ±4.6 GPa	50.62	45.66	51.70

4.2.4 Locating Uncovered CF Threads

When the CF threads were placed/dropped onto the epoxy covered SEM stub it looked like the majority of them were uncovered, but viewing the stub with the SEM quickly dispelled this initial assumption. Even though the epoxy had been

applied very sparingly, the majority of CF threads had become encased in the epoxy. It became evident most uncovered threads were located near the edges of the SEM stub. This is hypothesized to be because the epoxy was the thinnest at the edges. In the center, though the epoxy may have been thin, it was not less than the thickness of a CF thread. A search pattern for finding uncovered CF threads was developed and involved starting on the edge of the SEM stub and rotating the SEM stub within the instrument to ensure the entire outside of stub was checked. The majority of threads measured had half of their length completely covered with epoxy and the other half protruding out from the encased epoxy with only a minimum amount of epoxy adhering it to the SEM stub underneath. These threads then could be cut at the point where they were encased in epoxy leaving a section of CF thread uncovered to be measured by the AFM.

4.2.5 Cutting Carbon Fiber Threads with a FIB

In addition to ablating sizing, adhesive, and other contamination from the CF threads, the FIB was also used to cut threads to a length of less than 300 µm. Figure 23 is a good example of how a cut fiber looks once the FIB has made its way completely through. What then was needed to be investigated was if the modulus of the thread changed depending on the distance of the measurement from the cut position. Once it was ensured that the measurements met the selection criteria discussed in Section 4.3.2, it was observed that there was no statistical difference between the transverse moduli measured within 20 µm of a FIB cut and the transverse moduli measured 200 µm away from a FIB cut. In fact, some of the values which were used to calculate the average modulus for each thread came from sections near the cut and away from the cut. Table 2 demonstrates how similar moduli measured are regardless of their distance from a cut in the CF thread. Like the moduli values presented in Table 1,

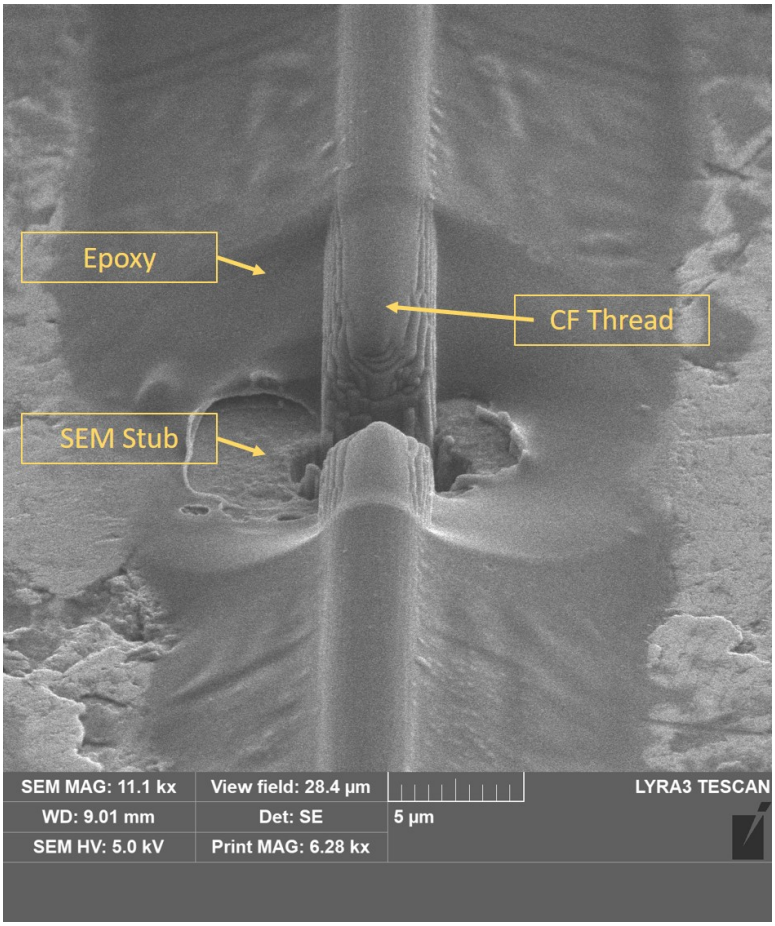

Figure 23. A section of CF thread cut by the FIB.

this data was collected with the same tip for consistency.

Table 2. Comparing the effect on the modulus when measuring moduli near a cut versus away from the same cut (CF Model IM9/G-12k).

Location of Section Measured	#1 (GPa)	#2 (GPa)	#3 (GPa)
Near a cut (within 20 µm) ±4.5 GPa	38.11	39.97	59.11
Away from a cut (at least 200 µm) ±4.2 GPa	38.07	39.33	51.12

4.3 Transverse Modulus Results and Data Processing

4.3.1 Raw Measured Transverse Modulus Values

Upon completing over 100 measurements (each measurement is 16k+ data points), the results in Table 3 were recorded with only the removal of measurements which had a recorded negative height or deformation as these represented non-real data. These values were also taken from a mixture of different lengths of CF threads. Some threads were only 50 µm long and others were closer to 800 µm in length. There was no statistical difference between the transverse moduli measured from a long CF thread from a shorter CF thread. This is because the actual measured area was at most 1 μm^2, meaning the measurement was too localized to be affected by the different lengths of the thread. From these values it was determined that a finer selection criteria needed to be implemented to reduce the standard deviation (also known as uncertainty for this project) associated with each CF thread's average modulus. The uncertainty was calculated as the standard deviation between each average CF thread moduli recorded per thread. If 28 measurements were taken, then the standard deviation between those 28 average moduli is defined as that thread's measured uncertainty. This was decided upon as Frey used a similar method and his code was re-purposed for this project [16].

Table 3. Raw data measured from five different CF threads.

CF Thread Model Name	HM63	AS4D	IM9/G-12k	AS4GP12k	Field Collected Sample
Longitudinal Modulus (GPa)	434.00	241.00	255.00	231.00	230.00
Number of Measurements Taken	28	43	48	24	15
Transverse Modulus Measured with FIB Method (GPa)	39.39	52.04	58.84	37.68	50.66
Percent Uncertainty with FIB Method	19.0	29.9	19.2	17.7	9.4

4.3.2 Determination of Measurement Selection Criteria

After conducting over 100 usable modulus measurements of five different types of threads, criteria were developed to determine what measurements to include or exclude. This was required to ensure only data which represented physical reality, met theoretical expectations, and was reproducible was used.

The first exclusion criterion was from the Bruker AFM technical manual [53]. If the height or deformation average value was negative for any given measurement, that data was immediately excluded as negative numbers in these data channels correlated to a physically impossible reality. This occurrence happened in less than 5% of all measurements taken, and coincided with a worn tip. As previously mentioned, this exclusion criterion was already implemented prior to the formation of Table 3.

The second exclusion criterion was based on observation of the modulus and height AFM data channels. If the modulus or height data windows showed streaks or were not homogeneous it pointed to either issues with the tip, potential defects within the thread itself, or the thread was not laying flat. This occurred in approximately 15% of measurements. When this happened it also coincided with either a negative height as mentioned previously or an unacceptable skew value that will be discussed later in this section. The reason why the percentage of times this occurred is only an approximation is because some measurements would be stopped before being completed as the data was being evaluated in real time and it was not recorded. When a non-homogeneous image of the surface was recorded, the area to be measured would

be offset by 100 nm and measured again. If another non-homogeneous image of the surface was collected the tip would be changed if the tip had been used numerous times or a new section of the thread would be measured.

The third criterion involved observing each measurement's data histogram and evaluating its skewness. Only measurements that had a histogram skewness value between -0.5 and 0.5 were used. This ensured that normal distribution statistics such as mean, standard deviation, and mode were accurate. If a measurement recorded had a skewed value less than -0.5 or greater than 0.5 then the average modulus calculated would not represent the true average. Skewness and the importance behind it was discussed in greater detail in Section 2.7.1.

The fourth criterion involved how to determine, out of all the measurements taken, what best represented a given CF thread's transverse modulus in GPa. It was determined the most precise representation of the modulus was the average of the highest five moduli (in GPa) measured. The standard deviation between the top five moduli is reported as the uncertainty or relative error. For clarity's sake, it must be annotated here that each of the five moduli which contributed to this average was itself an average of the 16k+ moduli data points collected in a single measurement. Because of the reliance on averages, it was critical that the skew criterion outlined in the previous paragraph was followed. This method of determining the modulus of a CF thread, based on the data available, was also used by Frey in 2021 [16]. Since the modulus of the CF thread is relative, the data recorded was not necessarily a representation of the true modulus of the thread; thus, precision was the goal. Furthermore, five measurements was the number chosen to average due to the role of tip wear on the modulus measurements. A brand new tip can reliably take 6-8 measurements without having to re-calibrate the tip and this also allows for one or two measurement failures. Sometimes, more measurements could be collected; but five was a number

which could be confidently achieved with every new tip. The logic behind using the highest averaged five moduli was based on the fact that each CF theoretically has a modulus ceiling that cannot be exceeded. Different variables such as if the CF thread is set at an angle, contamination on the thread, defects within the CF thread, or a dull AFM tip can contribute to the measured modulus being lower. However, none of the aforementioned occurrences could produce a higher modulus, making an average of the top moduli measured the best way to characterize a CF thread's transverse modulus. The only way a measured modulus could be higher than the CF thread's modulus is if a very hard piece of debris covered the CF thread and that debris was measured by the AFM. The epoxy used had a much lower modulus than the thread, and no other materials were used in this experiment, logically making the highest moduli measured an identifying characteristic of the CF thread.

4.3.3 Impact of AFM Scanning Rate on Modulus Distributions

Early in this experiment, when superglue was still being used as an adhesive, horizontal tip crashes were not uncommon as discussed in Section 3.1.4. In order to remedy this, a slower scanning rate was instituted, moving from a 0.250 Hz scan rate to a 0.001 Hz scan rate. This reduced the horizontal tip crash by 50% and improved an individual measurement's distribution standard deviation by approximately 3-4 GPa. This was because the tip was moving more slowly from point to point so that the measurements were more precise and the variance subsequently reduced. When the FIB method was being developed and the two-part epoxy was being used, the scan rate was initially maintained at 0.001 Hz. Due to time constraints of the project, the scan rate was then increased to 0.250 Hz to investigate if the two-part epoxy would also cause the same number of horizontal crashes. The horizontal tip crashes did not happen; and since the 0.250 Hz scan rate reduced the measurement time by 50% (30

minutes to 15 minutes), this scan rate, was used for the majority of measurements taken. With the increase in the scan rate the standard deviation did increase by an average of 1-2 GPa per modulus measurement; but the trade off was necessary. If more time had been available, the slower scan rate would have been utilized for all measurements. A cost/benefit analysis was conducted, and gathering data at the expense of a slightly larger variance per measurement was determined to be in the best interest of the project.

4.3.4 Rejection of AFM Transverse Modulus Output

As mentioned previously, the AFM output is 16,384 data points per measurement and each measurement records a transverse modulus in units of MPa. The Bruker Analysis software converts all data points into a histogram that is a representation of all modulus measurements in a single area as shown in Figure 24. One method

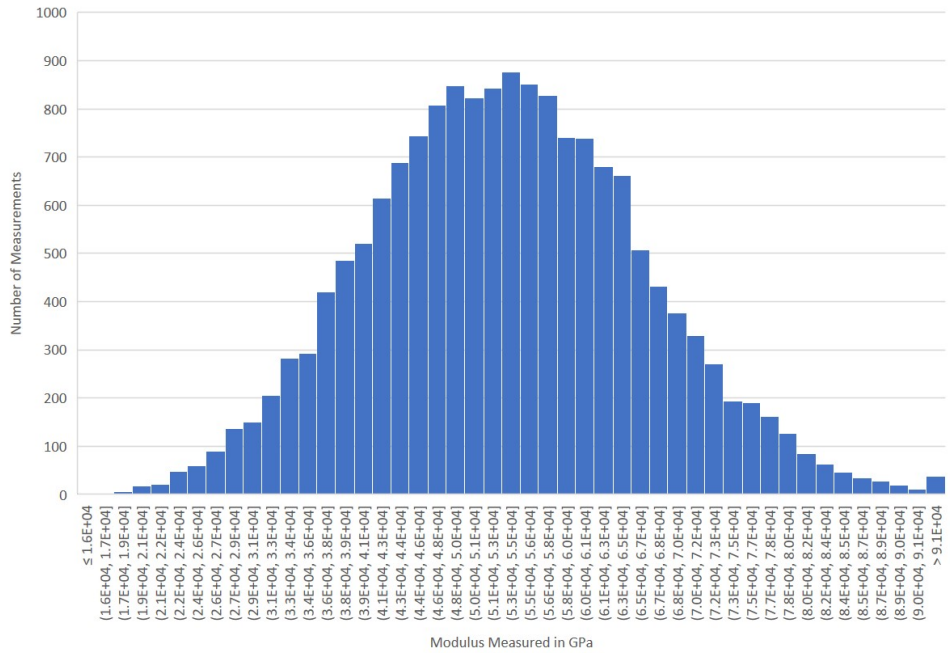

Figure 24. Example of a typical output of modulus measurements in histogram format.

attempted and ultimately rejected, was to take the value at the peak height of the modulus histogram as a representation of the entire measured area. But upon digging into the histogram's physical meaning a little deeper, the peak height only represents less than 1,000 data points. Thus, the most common modulus measurement per area scanned was only a representation of approximately 5% of the total measured area. For this reason, it was decided to use the average modulus as the measurements selected were Gaussian based on the skewness test conducted. An example of four of the threads histogram data compared with a Gaussian distribution can be seen in Figure 25.

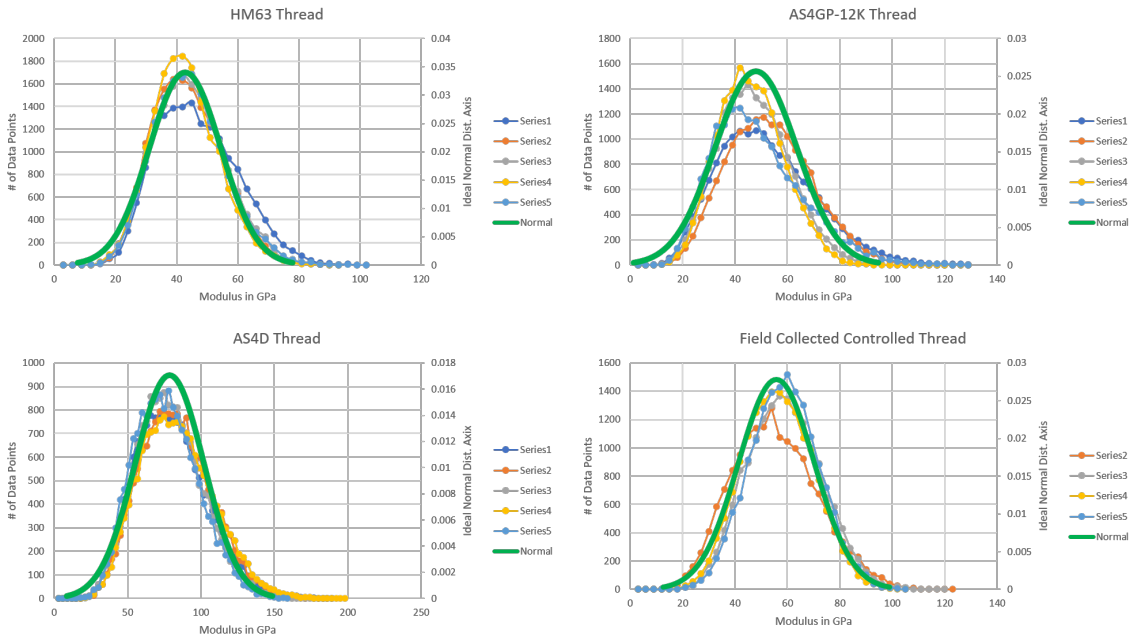

Figure 25. Highest five measured moduli distributions for four CF threads measured in this project compared to a normal distribution (skew value equal to 0).

4.3.5 Impact of Selection Criteria on Results

By implementing the selection criteria outlined above and selecting the highest five average moduli measured (5 separate scans of 16k+ data points each), the uncertainty (standard deviation) was between 2.4% and 5.8% depending on the fiber. The five measurements that had the highest average transverse modulus in GPa for each fiber and their accompanying uncertainty (standard deviation between the five averages) can be seen in Table 4.

Table 4. Average modulus from the top five measurements with uncertainty.

CF Thread Model Name	HM63	AS4D	IM9/G-12k	AS4GP12k	Field Collected Sample
Transverse Modulus Measured with FIB Method (GPa)	42.80	78.64	66.43	47.94	55.77
Percent Uncertainty with FIB Method	3.18	3.37	4.74	5.78	2.44

It is also important to note that comparisons between the results from this research project and previous research conducted are quite difficult to make since the sample preparation procedure was completely different. It does, however, highlight the difference that rastering the CF threads with a FIB makes when measuring the transverse modulus. It is clear to see all modulus values measured without the use of a FIB (previous research) are quite a bit lower, further supporting the hypothesis that rastering a CF thread prior to measuring its modulus makes a difference. The comparative results are shown in Table 5. For completeness, the modulus of the superglue which was used in the previous project was measured and compared to the modulus of the two-part epoxy used in this research project. Both adhesives were within a standard deviation of each other, averaging between 7-8 GPa. The sizing material on the CF threads could not be positively identified it was not possible to record a modulus for sizing in this project. It would be ideal to acquire a sample of the sizing material from the manufacturer to test but that was not possible within the scope of this research project.

Table 5. Comparing transverse moduli from a previous research project[16] with the longitudinal moduli and the moduli measured in this project.

CF Thread Model Name	HM63	AS4D	IM9/G-12k	AS4GP12k	Field Collected
Previously Measured Transverse Modulus (GPa)[16]	15.94	20.05	20.53	20.03	N/A
Transverse Modulus Measured with FIB Method (GPa)	42.80	78.64	66.43	47.94	55.77
Percent Uncertainty with FIB Method	3.18	3.37	4.74	5.78	2.44

4.3.6 Longitudinal Modulus vs. Transverse Modulus

Figure 26 shows how the transverse modulus compares to the respective CF thread's known longitudinal modulus. The CF thread 'field collected' is an export

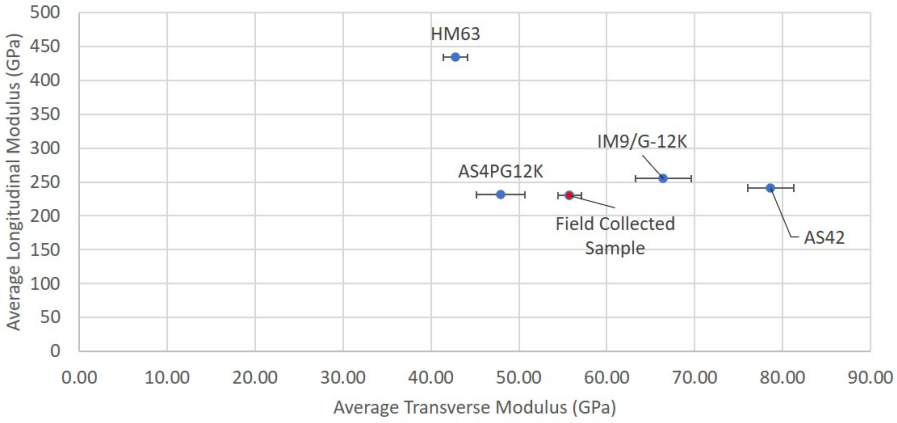

Figure 26. Manufacturer published longitudinal modulus plotted versus the relative transverse modulus measured in this research.

controlled sample that was taken from a post fabrication CF item; this particular fiber has the distinction of having only a 2.44% standard deviation (uncertainty) between the top five average moduli. In fact, this fiber was measured a total of 15 times and if all of those measurements were counted the standard deviation would only have increased to 9%. All other threads had an overall standard deviation of at least 17% without introducing any selection criterion as is shown previously in Table 3.

4.3.7 Correlation between Deformation and Modulus

An additional validation step to ensure the data collected was theoretically reasonable involved examining the correlation between deformation height and modulus. At first, the average modulus was plotted against the average deformation height to see if a linear relationship existed. What was found was some threads had a better linear relationship than others with an R^2 values ranging from 0.2 to 0.8 (an example of one thread's plot can be seen in Figure 27.

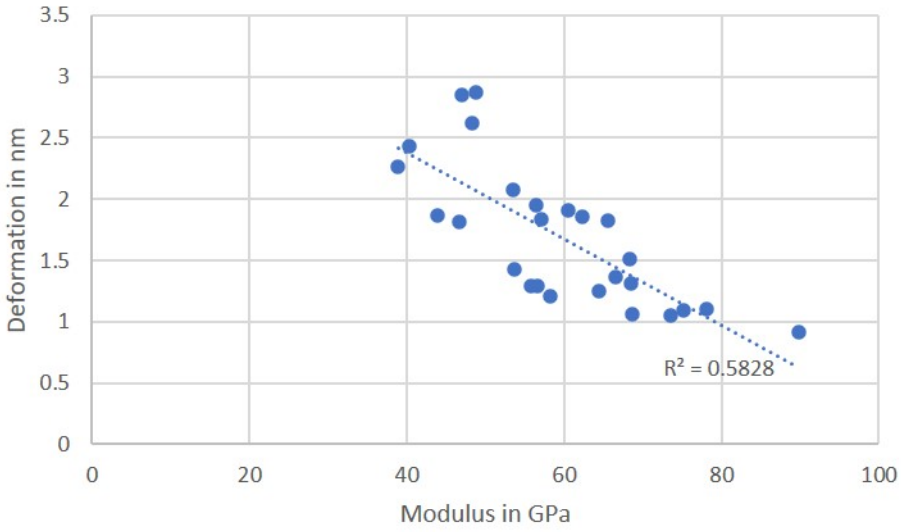

Figure 27. One CF thread's moduli measurements compared to its deformation height.

If the relationship was not inversely and linearly related, then there may be an issue with what equation was actually being implemented by the AFM software to solve for Young's modulus. To solve this issue, it was thought that since the average values for modulus and deformation were being used for Figure 27 and these averages were calculated from a distribution, that was not perfectly normal. This could cause issues with the overall linear relationship. To better check the data, it was determined that one individual measurement needed to be plotted and see if a linear relation-

ship existed. Using Excel's ANOVA program, which was able to compare moduli recorded at discreet deformation intervals, it was clear a linear relationship existed with an average R^2 of over 0.90. An example graph can be seen in Figure 28. This result made complete sense and confirmed the data collected was valid. Averages can be deceiving, especially when the distribution is not perfectly normal and trying to compare the average of two separate distributions becomes even harder as the likelihood those distributions perfectly line up is not probable. If the distributions do not look the same and one is skewed to the left and the other is skewed to the right, then plotting those averages represents data which is not true. By examining one individual measurement and using an ANOVA test to see how the modulus correlates to the deformation, it was easy to see the values matched the theoretical expected trend. Since Young's modulus inversely relates the deformation depth to the modulus as can be seen in Equation 4, it is important that the modulus measurements followed this theoretical expectation. This in fact became a final check to ensure the top five moduli chosen to represent each fiber's transverse modulus maintained a near linear relationship (R^2 value greater than 0.90) between the deformation depth and the modulus.

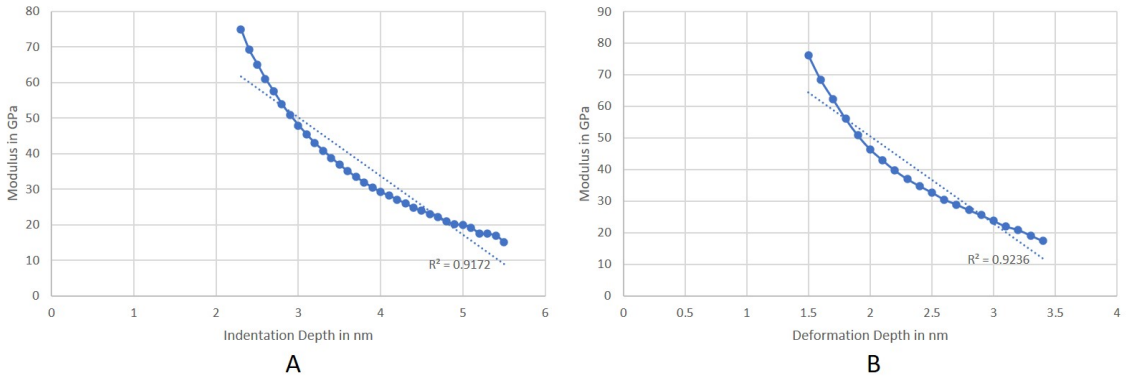

Figure 28. A: One measurement's modulus and deformation data channels plotted; B: One measurement's modulus and indentation data channels plotted.

4.3.8 ANOVA Testing Results

As stated in the previous section, an ANOVA test was conducted using Microsoft Excel's ANOVA testing package; and it was determined that there was a correlation between Deformation, Indentation, and Adhesion as it related to the measured modulus by observing the graphical representation. As the indentation and deformation height increased, the average modulus decreased; and as the average adhesion force increased, the measured modulus also increased. This was determined by binning the deformation, indentation, and adhesion data channels into discrete bins, observing the average modulus which corresponded, and plotting both numbers as is seen in Figure 28. However, the variance of the modulus was so large for each discrete bin (greater than 9 GPa) that the subsequent statistical P-value associated with the conducted ANOVA test was equal to 0; the only information gained from the ANOVA test was a general correlation between the modulus and the deformation, indentation, and adhesion data. It would have been ideal to know how each of these factors impacted the modulus (i.e. how much the deformation height would have to change to change the modulus by 1 GPa) but because of the wide variance in each data set no conclusions could be made.

4.4 Explanations for Inconsistent Measurements for PAN CF

Previous work has shown that fibers with a low longitudinal tensile strength have a high transverse modulus and vice versa [16]. No solid correlation between the two was found based on the recorded measurements from this project as can be seen in Figure 26. The lowest longitudinal modulus did have the highest transverse modulus while the highest longitudinal modulus did have the lowest transverse modulus, but the three other fibers which fell in between were not consistently staggered as may be expected. Possible reasons for this inconsistency could be a number of things. The

particular fibers measured were old and had started to degrade, the threads that were measured could be on an imperceptible angle causing the modulus to be lower, or the the measured transverse modulus of an individual thread by itself is not same as the transverse modulus of a tow. It is also possible that even though many measurements were taken, the best representation of the modulus was still not measured. CF can be manufactured for a particular purpose and with particular specifications; and though the general thought is CF with high longitudinal modulus should have a low transverse modulus, this is not a hard and fast rule. It is possible that the CF threads tested in this research project simply do not conform to the observations made by a research group relating a CF thread's longitudinal modulus to its transverse modulus.

4.5 Comparing the Modulus Distribution Skewness

The skewness of all distributions were evaluated and any measurement that had a skewness less than -0.5 and greater than 0.5 were discarded (roughly 10%). However it was interesting to note the range and uncertainty between all skewness measurements to see exactly how close to Gaussian the distributions were. Some fibers were much closer to Gaussian than others as can be seen in Table 6.

Table 6. Average skew value for each CF thread's modulus distribution and its standard deviation.

CF Thread Model Name	HM63	AS4D	IM9/G-12k	AS4GP12k	Field Collected Sample
Average skew value of the modulus distribution	0.38	0.36	0.36	0.45	0.18
Standard deviation of the skew value	0.04	0.05	0.09	0.20	0.10

The field collected, export-controlled sample had the most Gaussian distribution; and even with its associated standard deviation, it still had the least amount of skew to its distribution. As mentioned in Chapter 2, the tensile strength of materials has been associated with a normal distribution and it could be hypothesized that a normal distribution to represent the transverse modulus could also be appropriate. If

the distribution of the modulus measurement is skewed to the right than a log-normal fit would be most appropriate, but this model makes averages and standard deviation more complicated. Complicated does not mean impossible but finding distributions which were closer to normal was chosen because it was one way to narrow down the data and a previous study had linked normal distributions to tensile strength, hardness, and fracture toughness [49].

4.6 Measuring Pitch CF Threads

Measuring the modulus of a pitch fiber was attempted using the developed method with little success. Due to the physical differences between pitch and PAN threads, the ridges on the pitch fiber as shown in Figure 29 made it impossible to ablate the epoxy. Because the FIB works by ablating layers of a material, it would ablate

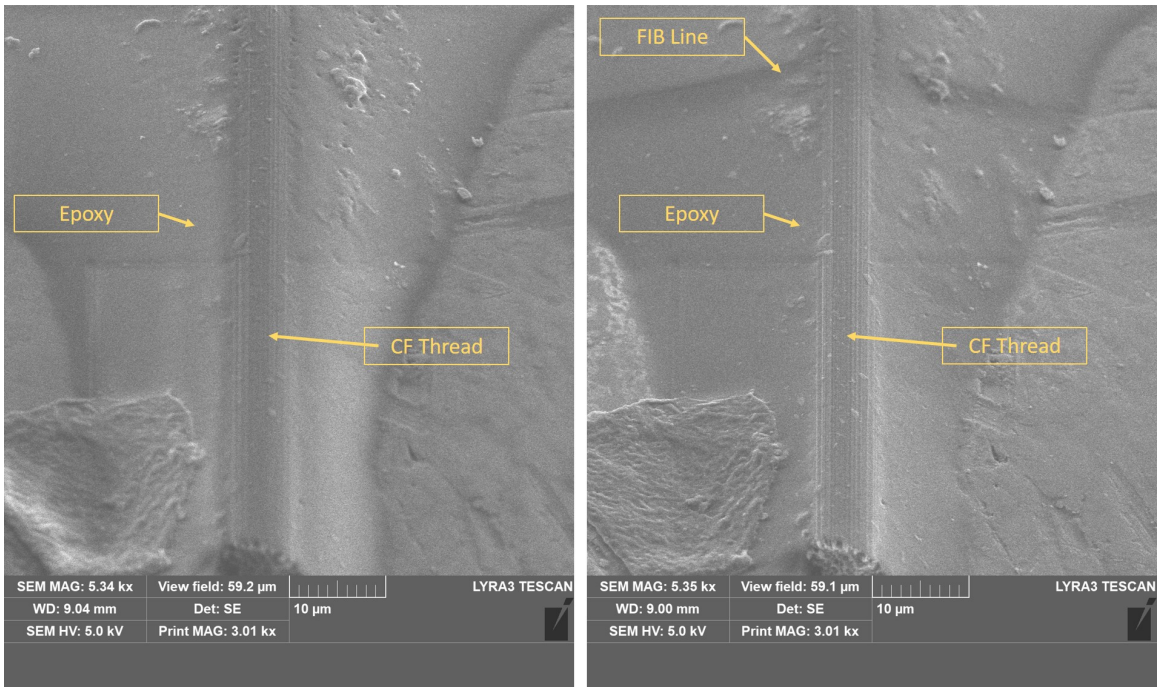

Figure 29. Pitch CF thread before (left) and after (right) being ablated by the FIB

away the peaks and leave the CF thread even with the epoxy. Figure 30 is an image taken by the AFM showing the ridges and epoxy trapped in the resulting valleys on a 2.25 μm^2 area. This resulted in irregularities in the modulus because epoxy mixed

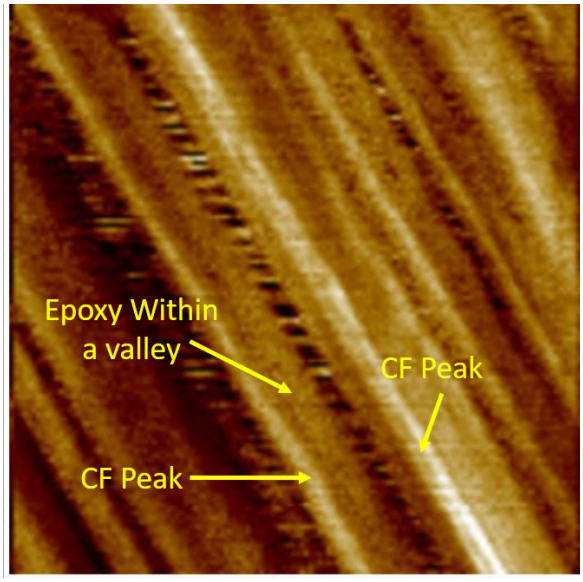

Figure 30. PeakForce mapping of a 2.25 μm^2 area on a pitch CF thread.

in with the CF thread to give an inaccurate measurement. Since the integrity of the CF is paramount when measuring the modulus, any damage to the CF thread with the FIB would render the measurements useless. The layered structure of pitch CF creates the peaks seen in Figure 29 and Figure 30, which made ablating only the epoxy impossible due to how the FIB removes material in layers. PAN CF, on the other hand, has a smooth surface, making it quite easy to only ablate the epoxy until the CF thread is exposed. It was therefore decided to focus solely on PAN fibers for this research project as the method could be reliably reproduced.

4.6.1 Additional Issues with Measuring the Transverse Modulus with the AFM

Measuring the transverse modulus of the CF threads with the AFM was not without its problems. Learning how to identify objects and features on the PeakForce image display takes time. As the experiment progressed it also took experience to know where certain processes could be streamlined and how to interpret different errors as well as overcome them. A common error encountered was replacing the AFM tip; and after calibrating the deflection and spring constant, the tip characterization algorithm would return a tip radius value of over 25 nm. Since this tip was taken straight out of the box and should have a nominal value of 8-10 nm, this was a completely unacceptable radius. To make the problem more complicated, the Peakforce image produced of the tip characterization standard had very good resolution indicating a sharp tip. To try and solve this issue, 9 nm was entered into the tip radius input box even when the software said the tip radius was 25 nm. This method was ultimately not successful because entering a smaller tip radius artificially increased the modulus output of the surface being measured. A test was conducted where a modulus was measured with a brand new and properly characterized tip at 8.6 nm, and the modulus was recorded as 44 GPa. The same exact surface was measured again, but this time the tip radius was arbitrarily increased to 11 nm and the modulus output was subsequently reduced to 40 GPa. This indicated that the modulus was in fact driven by the tip radius entered by the user and reflected the implementation of Equation 4. It was then thought that maybe the same tip radius size should be decided arbitrarily regardless of what the tip characterization program stated the radius to be since all of the measurements in this project were relative. This posed a problem because there would be no way to calculate the uncertainty associated with entering a tip radius arbitrarily. Looking through the measurements that had

already been taken, it was determined that similar moduli had recorded with different tip radii entered and using the prescribed method by the Bruker user manual was ultimately the best plan of action. Consequently, whenever the tip characterization software would output a tip radius which was outside of the nominal standards for Bruker's tips, the computer and software were restarted and the tip was characterized again. If this this did not fix the problem the tip was exchanged.

4.7 Summary of Results and Analysis

4.7.1 Comparing CF Thread's Transverse Moduli

After compiling all the data, it is evident that the length of the thread does not change the measured modulus of that thread. Measuring 20 μm from a cut in the thread and 200 μm from that same cut makes little difference as the range of modulus recorded near a cut was well within a standard deviation of the range of modulus recorded away from the cut. It was also confirmed that rastering a CF thread with a FIB results in a higher measured modulus due to the fact the fiber is exposed and being measured directly. Though it cannot be 100% confirmed that the threads measured did not have any adhesive or sizing on them, it can be confirmed there were no large imperfections visible on the thread. Each thread was also measured using the same exact criteria to ensure maximum similarities in the method. Logically, a CF thread has a theoretical ceiling that cannot be surpassed; but any kind of imperfection, contamination, or defect could potentially lower the measured modulus. Lower moduli will always be present, but it is physically impossible, within the procedure used for this project, to contaminate or otherwise influence a CF thread so as to measure a CF thread at a higher modulus that what is physically possible. To manufacture or otherwise influence the modulus measurement in this way, a material which is harder than the CF thread would have had to adhere itself to the CF sample and remain

unablated and undetected. As no materials were present in the lab which had a higher theoretical transverse modulus than the CF thread, this likelihood can be assumed to be zero. However, even with this new approach interpreting the measurements, the CF threads measured cannot be differentiated simply by their transverse modulus. Two of the threads HM63 and AS4GP12k overlap when the uncertainty is taken into consideration. Though all threads measured had different averages, each average was not outside another CF thread's average standard deviation. This made the process of identifying a type of thread by only the transverse modulus impossible.

4.7.2 Physical Reason for Variations in Modulus Measurements

When a section of CF thread was measured as discussed in Chapter 3, one measurement would be taken and then the tip would be offset by 100 nm to 1 µm before being engaged again. A grouping of 5-8 measurements within an area of 1-5 µm would return values within 1-5% of each other. Analyzing this change in moduli was important to try and understand the physical influences causing the variance. Working from the theoretical foundation, the change in the CF thread's modulus is based on the radius of the AFM tip and the depth of deformation caused by the tip. Depending on the material the tip is in contact with, the deformation will be different since the force applied has remained the same at 500 nN. A section of the CF thread that is covered with adhesive will allow the tip to deform its surface further than a section of CF thread that is bare. Additionally, the very center of a CF thread will theoretically have the highest modulus based on the fact a material is always going to be stiffest where there is more mass. Therefore, any measurement off-center should theoretically have a lower modulus. Since the off-center distance is only a matter of nanometers, a large difference in moduli should not be detected; but it does logically make sense to have a range of moduli within a measured area. There is no exact way

to tell whether or not the highest moduli recorded in a set of data is due to it A) being closer to the center of the CF thread, B) an area not covered by any adhesive, C) both; the data point is closer to the center and is also not covered with adhesive.

4.7.3 Characteristics of Export Controlled CF vs. Non-Export Controlled CF

One interesting discovery was that the field collected, export-controlled CF thread had a much higher uniformity when it came to its measured modulus than the commercially available CF threads. This was deduced because the uncertainty associated with the controlled CF thread was between 0.75% and 3.34% lower than the uncertainty associated with a commercially available thread. Additionally, the controlled CF thread's probability distribution associated with its measured modulus was 0.2 to 0.41 less when comparing skewness values of each of the other thread's distribution. This hypothesis makes logical sense since export-controlled CF is used for mechanically stressful purposes with low tolerances for failure. It therefore can be hypothesized that the quality of the CF is potentially more important than even the total tensile strength or transverse modulus when it comes to evaluating if a CF thread is either export controlled or not. Though this is just a hypothesis which would require more testing, it is an observation which was not predicted or expected.

V. Conclusion

5.1 Summary

This research project began with the goal of demonstrating that a micron size CF thread would maintain the same modulus measurement as a larger sized CF thread using a method which was previously developed [16][15]. It ended with the development of a new method of mounting CF threads, a new method for preparing the CF threads to maximize the modulus measured, provided data which indicated the length of the CF thread did not impact the modulus measurement, and also gave insight into a difference between export controlled CF and commercially available CF thread.

5.1.1 New Mounting Technique

After experiencing issues with separating individual CF threads from a section of tow due to static electricity, the introduction of moisture to the separation method improved the efficiency and effectiveness by 50%. It was also found that using two-part epoxy instead of generic superglue not only allowed for more time to evenly spread the adhesive but also place the threads on the adhesive because the epoxy had a longer cure time.

5.1.2 Positive Impact of the SEM/FIB Instrument to the Procedure

This research project introduced the use of an SEM to observe the sample to ensure it was not covered with adhesive and introduced a FIB to cut CF threads to less than 300 µm in length. However, it was noted that all threads mounted had some degree of contamination; and the FIB was employed to ablate these contaminates off the surface. The difference between the modulus from a surface which has been

exposed to the FIB and one which had not been exposed was roughly 55%. This means all previous research projects which did not use a FIB to mill down the surface probably had an additional source of uncertainty due to the presence of contaminants. It cannot be overstated how crucial the SEM was to this research project because, without it, an uncovered section of CF thread was impossible to identify. With the SEM, threads were identified and cleaned with the FIB prior to being analyzed with the AFM.

5.1.3 Impact of Thread Length and FIB cut on the CF Thread's Transverse Modulus

After analyzing the modulus of five different model CF threads, it was determined that the length of the CF thread did not impact the measured modulus. To further examine the impact of length, measurements were also taken close to where the CF thread had been cut with the FIB (within 20 µm) and far from the FIB cut (minimum of 100 µm); and the results were within one standard deviation of each other. What was determined to have the biggest impact on any modulus measurement was the amount of contamination on the CF thread. Any adhesive, dirt, or unknown debris would cause a variation in the measured modulus. Since the area measured in this project was only at a 1 μm^2 area, it did not matter if a CF thread was 300 µm long or 800 µm long; the measured area was too localized for the length to impact.

5.1.4 Difference Between Export Controlled and Non-Export Controlled CF

This research only identified one possible way to determine if a CF thread may be export-controlled or not. The variation between measured moduli for an export-controlled CF was approximately between 6.86% and 0.73% less than the variation in

the measured moduli of the commercially available CF. Additionally, the distribution of the data collected from an export-controlled thread was significantly more Gaussian as was proven by looking at the skew values of each modulus distributions. The skew value for the export-controlled thread was 0.18 while the next best skew value from a commercially available thread was 0.38, more than double than that of an export-controlled thread. These two observations led to the hypothesis that the determining factor in export controlled or not controlled CF threads does not lie in the actual transverse modulus value, but rather, the amount of variation measured. It is logical that CF produced with the express purpose of being used in demanding, expensive, and controlled environments would have to have a higher quality due to the negative impacts failure would bring.

5.2 Future Work

5.2.1 Expansion of CF Thread Testing

To confirm the results of this project, many more PAN controlled and commercially available CF threads would have to be tested to see if the theory hypothesized here is correct. Only having one controlled CF thread and comparing it against four commercially available threads is not enough data to positively confirm this theory. PAN and Pitch controlled CF threads may also be different when it comes to differences in export controlled and not controlled, but it is estimated that the uniformity of a controlled fiber is paramount due to the stringent requirements of the application.

5.2.2 Raman Spectroscopy and Electron Dispersive Spectrometry (EDS)

Raman spectroscopy also may be another technique which may be able to differentiate CF threads from each other based on their chemical structure (ordered and non-ordered carbon). Previous researchers have noticed the ratio between the G (or-

dered carbon) and D (disordered carbon) bands vary with each type of CF tested. If export and non-export controlled CF could be cataloged by their G and D band ratios, it is possible Raman spectroscopy could be used to test random micron sized samples to ascertain if they are controlled materials or not. Using Raman would also cut out a large amount of sample preparation as the CF threads could simply be taped to a glass slide instead of being adhered with epoxy. Additionally, if enough testing is conducted then a link between the G and D band ratios and the tensile strength and/or modulus may be discovered. If this is proven then by using Raman spectroscopy an unknown sample of CF thread may be able to be characterized not only as controlled or not controlled but also identify a range of values for its tensile strength and modulus.

EDS has the ability to characterize a sample by identifying its elemental composition. Instead of using photons (lasers) to excite the material, EDS uses electrons. The data output is purely based on the elemental composition of the material as opposed to Raman which probes the intermolecular forces binding the molecules together. EDS requires a lot less knowledge of lasers, wavelengths, and less safety precautions. Both instruments provide slightly different types of data, but both would do an excellent job of characterizing CF threads. The possibilities are potentially groundbreaking.

5.2.3 Microstructure and Crystalline Size Study

In Section 2.3, it was noted that a research group had conducted a study and had linked the microstructure and crystalline size to the strength and modulus of a CF thread. This could potentially be another avenue to pursue for future work. If an empirical relationship could be developed between the microstructure and crystalline size to a specific strength and modulus, it would eliminate the need for individually testing each fiber using a PeakForce tapping technique. A CF thread could simply be

cut and be observed using a SEM. It would require developing a relationship between the measured crystalline size and microstructure to the manufacturer's strength and modulus limits. The goal would be to use an SEM to characterize a CF thread's strength and modulus based only on its crystalline size and microstructure.

Bibliography

1. P. Bhatt and A. Goe, "Carbon fibres: Production, properties and potential use," *Material Science Research India*, vol. 14, pp. 52–57, 06 2017.

2. J. Gross, *High Performance Carbon Fibers Commemorative Booklet.* Bethsada, MD: American Chemical Society, 2003.

3. M. Whelan, "Arc lamps," Schenectady, NY. [Online]. Available: https://edisontechcenter.org/ArcLamps.html#works [Accessed: 10/28/21]

4. CFCCarbon, "Manufacture of rayon-based carbon fibers," Beijing, China, 2021. [Online]. Available: https://www.cfccarbon.com/news/manufacture-of-rayon-based-carbon-fibers.html [Accessed: 11/27/21]

5. I. Toray Composite Materials America, "High modulus carbon fibers," Japan, 2021. [Online]. Available: https://www.toraycma.com/products/carbon-fiber [Accessed: 10/12/21]

6. CFCCarbon, "Comparison on modulus and strength of pan based and pitch based carbon fibers," Beijing, China, 2021. [Online]. Available: https://www.cfccarbon.com/news/comparison-on-modulus-and-strength-of-pan-pitch-based-carbon-fibers.html [Accessed: 11/27/21]

7. E. N. Society, "Gas centriuge process," Brussels, Belgium, 2020. [Online]. Available: https://www.euronuclear.org/glossary/gas-centrifuge-process/ [Accessed: 2/18/22]

8. Federation of American Scientists, "How a centrifuge works," Washington, DC, 2021. [Online]. Available: https:

//fas.org/issues/nonproliferation-counterproliferation/nuclear-fuel-cycle/uranium-enrichment-gas-centrifuge-technology/centrifuge-works/ [Accessed: 10/12/20]

9. P. Omnes, "Numerical and physical comparisons of two models of a gas centrifuge." *Computers Fluids*, vol. 36, no. 6, pp. 1028 – 1039, 2007.

10. R. S. KEMP, "Gas centrifuge theory and development: A review of u.s. programs," *Science & Global Security*, vol. 17, no. 1, pp. 1–19, 2009.

11. R. W. Lyczkowski, "Nuclear chemical engineering," *AICHE Journal*, vol. 28, no. 4, pp. 702–702, 1982.

12. D. Albright and A. Stricker, "Iranian atomic energy organization attempted carbon fiber procurement," 2016.

13. W. Burr, "To "keep the genie bottled up": U.s. diplomacy, nuclear proliferation, and gas centrifuge technology, 1962-1972." *Journal of Cold War Studies*, vol. 19, no. 2, pp. 115 – 157, 2017.

14. N. S. Group, "Guidelines for nuclear transfers," June 2019. [Online]. Available: http://nuclearsuppliersgroup.org/images//2019NSG_Part_1.pdf [Accessed: 10/15/21]

15. L. Veigas, "Countering Proliferation: Carbon Fiber Characterization with PeakForce QNM," Master's thesis, Air Force Institute of Technology, 2020.

16. J. Frey, "Error reduction for the determination of transverse moduli of single-strand carbon fibers via atomic force microscopy," Master's thesis, Air Force Institute of Technology, 2021.

17. R. Guoqiang, "Carbon nanotube," Chicago, IL. [Online]. Available: https://www.britannica.com/science/carbon-nanotube [Accessed: 11/1/21]

18. D. Li, H. Liu, B. Chen, N. Dong, B. Lei, G. Ye, W. Jiang, Y. Shi, L. Yin, and G. Lai, "Amorphous carbon-induced surface defect repair for reinforcing the mechanical properties of carbon fiber," *Materials*, vol. 12, p. 1244, 04 2019.

19. H. Okuda, R. Young, D. Wolverson, F. Tanaka, G. Yamamoto, and T. Okabe, "Investigating nanostructures in carbon fibres using raman spectroscopy," *Carbon*, vol. 130, 2018.

20. S. A. Mirdehghan, *1 - Fibrous polymeric composites*, ser. The Textile Institute Book Series, M. Latifi, Ed. Woodhead Publishing, 2021.

21. K. Naito, Y. Tanaka, and J. Yang, "Transverse compressive properties of polyacrylonitrile (pan)-based and pitch-based single carbon fibers," *Carbon*, vol. 118, 2017.

22. C. World, "Materials processes: Fabrication methods," Cincinnati, OH. [Online]. Available: https://www.compositesworld.com/articles/fabrication-methods [Accessed: 10/24/21]

23. H.-w. He, F. Gao, and K.-x. Li, "Effect of epoxy resin properties on the mechanical properties of carbon fiber/epoxy resin composites," *International Journal of Materials Research*, vol. 104, pp. 899–902, 09.

24. P. Bhatt and A. Goe, "Carbon fibres: Production, properties and potential use," *Material Science Research India*, vol. 14, pp. 52–57, 06.

25. M. Company, "Reinforced plastic composites: Fiber sizing," Cincinnati, OH, 2021. [Online]. Available: https://www.michelman.com/markets/reinforced-plastic-composites/fiber-sizing/ [Accessed: 11/12/21]

26. F. Ibn Afzal, M. C. Saha, and M. C. Altan, "Effect of Sizing Removal Method and POSS Coating on Flexural Properties of Carbon Fiber Epoxy Composites," vol. Volume 9: Mechanics of Solids, Structures and Fluids, 11 2013.

27. MichelMan, "Fiber sizing," 2021. [Online]. Available: https://www.michelman.com/markets/reinforced-plastic-composites/fiber-sizing/ [Accessed: 12/3/21]

28. A. Zafar, F. Bertocco, J. Schjødt-Thomsen, and J. Rauhe, "Investigation of the long term effects of moisture on carbon fibre and epoxy matrix composites." *Composites Science Technology*, vol. 72, no. 6, pp. 656 – 666, 2012.

29. X. F. Wan, Y. L. Wang, F. G. Zhou, and Y. Z. Wan, "Moisture absorption behavior of carbon fiber-reinforced monomer casting nylon composites," *Journal of Reinforced Plastics and Composites*, vol. 23, no. 10, pp. 1031–1040, 2004.

30. G. Betz, "Sputtering by particle bombardment," *Acta Crystallographica Section A*, vol. 38, pp. 399–399, 05 1982.

31. P. Sigmund, "Mechanisms and theory of physical sputtering by particle impact," *Nuclear Instruments and Methods in Physics Research Section B: Beam Interactions with Materials and Atoms*, vol. 27, no. 1, pp. 1–20, 1987.

32. Q. Wu, M. Li, Y. Gu, S. Wang, and Z. Zhang, "Imaging the inter-phase of carbon fiber composites using transmission electron microscopy: Preparations by focused ion beam, ion beam etching, and ultramicrotomy," *Chinese Journal of Aeronautics*, vol. 28, no. 5, pp. 1529–1538, 2015.

33. S. Magni, M. Milani, C. Riccardi, and F. Tatti, "Fib/sem characterization of carbon-based fibers," *Scanning*, vol. 29, no. 4, pp. 185–195, 2007.

34. D. W. Collinson, R. J. Sheridan, M. J. Palmeri, and L. Brinson, "Best practices and recommendations for accurate nanomechanical characterization of hetero-

geneous polymer systems with atomic force microscopy," *Progress in Polymer Science*, p. 101420, 2021.

35. S. Duan, F. Liu, T. Petterson, C. Creighton, and E. Asp, "Determination of transverse and shear moduli of single carbon fibres," *Carbon*, vol. 158, 2020.

36. S. Reyntjens and R. Puers, "A review of focused ion beam applications in microsystem technology," *Journal of Micromechanics and Microengineering*, vol. 11, no. 4, pp. 287–300, July 2001.

37. N.-T. Nguyen, *Chapter 4 - Fabrication technologies*, second edition ed., ser. Micro and Nano Technologies, N.-T. Nguyen, Ed. Oxford: William Andrew Publishing, 2012.

38. F. Liu, S. Duan, and L. Asp, *Specimen Preparation for Transverse Modulus Measurement of Carbon Fibres Using Focused Ion Beam.* Melbourne, Australia: Engineers Australia, 2019.

39. R. Asmatulu and W. S. Khan, *Chapter 13 - Characterization of electrospun nanofibers*, ser. Micro and Nano Technologies, R. Asmatulu and W. S. Khan, Eds. Elsevier, 2019.

40. F. Braet and M. Radmacher, "Foreword to the special issue on afm in biology bionanomedicine," *Micron*, vol. 43, no. 12, p. 1211, 2012, special issue on AFM in Biology Bionanomedicine.

41. A. Zhou, H. Zhang, Q. Li, and L. Xiao, *AFM and Raman Spectroscopy, Applications in Cellular Imaging and Assays*, third edition ed., J. C. Lindon, G. E. Tranter, and D. W. Koppenaal, Eds. Oxford: Academic Press, 2017.

42. A. Bonyár, "Afm characterization of the shape of surface structures with localization factor." *Micron*, vol. 87, pp. 1 – 9, 2016.

43. N. Jalili and K. Laxminarayana, "A review of atomic force microscopy imaging systems: Application to molecular metrology and biological sciences," *Mechatronics*, vol. 14, pp. 907–945, 10 2004.

44. Y. Qiu, Y. Chen, G. G. Zhang, L. Yu, and R. V. Mantri, Eds., *Chapter 8 - Interfacial Phenomena*, second edition ed. Boston: Academic Press, 2017.

45. X. Kong, J. Deng, J. Dong, and P. H. Cohen, "Study of tip wear for afm-based vibration-assisted nanomachining process," *Journal of Manufacturing Processes*, vol. 50, pp. 47–56, 2020.

46. S. Ushiba, K. Masui, N. Taguchi, T. Hamano, S. Kawata, and S. Shoji, "Size dependent nanomechanics of coil spring shaped polymer nanowires," *Scientific reports*, vol. 5, p. 17152, 11 2015.

47. A. Paar, "Atomic force microscopy (afm)," Graz, Austria, 2021. [Online]. Available: https://wiki.anton-paar.com/en/atomic-force-microscopy-afm/ [Accessed: 10/14/21]

48. A. Millet, "A universal model for the log-normal distribution of elasticity in polymeric gels and its relevance to mechanical signature of biological tissues," *Biology*, vol. 10, p. 64, 01 2021.

49. T. Sakai, M. Nakajima, K. Tokaji, and N. Hasegawa, "Statistical distribution patterns in mechanical and fatigue properties of metallic materials," *Journal of The Society of Materials Science, Japan*, vol. 46, pp. 63–74, 1997.

50. NIST, "E-handbook of statistical methods," Washington, DC, 2013. [Online]. Available: https://doi.org/10.18434/M32189 [Accessed: 1/25/22]

51. Microsoft, "Skew function," 2021. [Online]. Available: https://support.microsoft.com/en-us/office/skew-function-bdf49d86-b1ef-4804-a046-28eaea69c9fa [Accessed: 2/18/22]

52. Y. Huang and R. Young, "Effect of fibre microstructure upon the modulus of pan- and pitch-based carbon fibres," *Carbon*, vol. 33, Issue, 2, 1995.

53. Bruker Corporation, "PeakForce QNM User Guide," 2011.

REPORT DOCUMENTATION PAGE

Form Approved
OMB No. 0704–0188

1. REPORT DATE *(DD–MM–YYYY)*	2. REPORT TYPE	3. DATES COVERED *(From — To)*
22–03–2022	Master's Thesis	Sept 2020 — Mar 2022

4. TITLE AND SUBTITLE

Analysis of Microscopic Carbon Fiber Fragments

5a. CONTRACT NUMBER

5b. GRANT NUMBER

5c. PROGRAM ELEMENT NUMBER

6. AUTHOR(S)

Scott, Zachary R., MAJ, USA

5d. PROJECT NUMBER

XXXXXX

5e. TASK NUMBER

5f. WORK UNIT NUMBER

7. PERFORMING ORGANIZATION NAME(S) AND ADDRESS(ES)

Air Force Institute of Technology
Graduate School of Engineering and Management (AFIT/EN)
2950 Hobson Way
WPAFB OH 45433-7765

8. PERFORMING ORGANIZATION REPORT NUMBER

AFIT-ENP-MS-22-M-109

9. SPONSORING / MONITORING AGENCY NAME(S) AND ADDRESS(ES)

Defense Threat Reduction Agency

10. SPONSOR/MONITOR'S ACRONYM(S)

DTRA

11. SPONSOR/MONITOR'S REPORT NUMBER(S)

12. DISTRIBUTION / AVAILABILITY STATEMENT

DISTRIBUTION STATEMENT A:
APPROVED FOR PUBLIC RELEASE; DISTRIBUTION UNLIMITED.

13. SUPPLEMENTARY NOTES

14. ABSTRACT

Carbon Fiber (CF) has different tensile strengths and transverse moduli depending on how they are fabricated. Some CF is export controlled as it can be used for weapons, spacecraft, or gas centrifuges for enriching nuclear fuel. This research project explored a new way to prepare micron sized single CF threads to measure their transverse modulus and compare the moduli of non-export controlled CF to that of an export controlled CF. Five total polyacrylonitrile (PAN) fibers were used in this project, one of which was an export controlled fiber.

15. SUBJECT TERMS

carbon fiber, atomic force microscopy, nuclear forensics, materials analysis

16. SECURITY CLASSIFICATION OF:			17. LIMITATION OF ABSTRACT	18. NUMBER OF PAGES	19a. NAME OF RESPONSIBLE PERSON
a. REPORT	b. ABSTRACT	c. THIS PAGE			Dr. Abigail A. Bickley, AFIT/ENP
U	U	U	UU	105	19b. TELEPHONE NUMBER *(include area code)* (937) 255-6565 x4555; abigail.bickley@afit.edu